


Comprehensive theory of the Lamb shift in light muonic atoms

K. Pachucki 

Faculty of Physics, University of Warsaw, Pasteura 5, 02-093 Warsaw, Poland

V. Lensky 

Institut für Kernphysik, Johannes Gutenberg-Universität Mainz, 55128 Mainz, Germany

F. Hagelstein 

*Institut für Kernphysik, Johannes Gutenberg-Universität Mainz, 55128 Mainz, Germany
and Paul Scherrer Institut, CH-5232 Villigen PSI, Switzerland*

S. S. Li Muli 

Institut für Kernphysik, Johannes Gutenberg-Universität Mainz, 55128 Mainz, Germany

S. Bacca 

*Institut für Kernphysik, Johannes Gutenberg-Universität Mainz, 55128 Mainz, Germany
and Helmholtz-Institut Mainz, Johannes Gutenberg-Universität Mainz, 55099 Mainz, Germany*

R. Pohl 

Institut für Physik, Johannes Gutenberg-Universität Mainz, 55099 Mainz, Germany

 (published 24 January 2024)

A comprehensive theory of the Lamb shift in light muonic atoms such as μH , μD , $\mu^3\text{He}^+$, and $\mu^4\text{He}^+$ is presented, with all quantum electrodynamic corrections included at the precision level constrained by the uncertainty of nuclear structure effects. This analysis can be used in the global adjustment of fundamental constants and in the determination of nuclear charge radii. Further improvements in the understanding of electromagnetic interactions of light nuclei will allow for a promising test of fundamental interactions by comparison with “normal” atomic spectroscopy, in particular, with H-D and ^3He - ^4He isotope shifts.

DOI: [10.1103/RevModPhys.96.015001](https://doi.org/10.1103/RevModPhys.96.015001)

CONTENTS

I. Introduction	2	N. Pure recoil $\sim(Z\alpha)^6$	9
II. Expansion of Energy in Powers of the Fine Structure Constant α	3	O. Radiative recoil $\sim\alpha(Z\alpha)^5$	9
III. QED Contributions to the Lamb Shift	5	P. Hadronic vacuum polarization	9
A. Electron vacuum polarization	5	Q. Combined electron and hadronic vacuum polarization	10
B. Light-by-light electron vacuum polarization	6	IV. Finite Nuclear Size Contribution	10
C. Leading recoil $\sim(Z\alpha)^4$	6	A. Leading finite size r_C^2	10
D. Relativistic correction with the one-loop electron vacuum polarization	6	B. One-loop electron vacuum polarization with r_C^2	10
E. Relativistic correction with the two-loop electron vacuum polarization	7	C. Two-loop electron vacuum polarization with r_C^2	10
F. Leading muon self-energy and vacuum polarization	7	V. Nuclear Structure Contributions	10
G. Next-to-leading muon self-energy and vacuum polarization	7	A. Two-photon exchange	10
H. Combined muon and electron vacuum polarizations	7	1. TPE in μH	11
I. Muon self-energy combined with the electron vacuum polarization	8	2. TPE in μD	12
J. Recoil $\sim(Z\alpha)^5$	8	3. TPE in μHe^+	13
K. Recoil with the electron vacuum polarization	8	B. Coulomb distortion correction	14
L. Nuclear self-energy	8	C. Three-photon exchange	14
M. Muon two-loop form factors and vacuum polarization	9	D. Electron vacuum polarization with TPE	14
		E. Muon self-energy and vacuum polarization with TPE	15
		VI. Summary	15
		Acknowledgments	16
		Appendix A: Subtraction of the Point Deuteron Amplitude	16
		Appendix B: eVP ⁽¹⁾ Correction with TPE on Single Nucleons	17
		Appendix C: eVP ⁽¹⁾ Correction with TPE on Different Nucleons	17

Appendix D: $eVP^{(1)}$ Correction with the Leading Polarizability	18
Appendix E: $\mu SE^{(1)} + \mu VP^{(1)}$ Correction with the Elastic TPE	18
References	19

I. INTRODUCTION

Two-body systems such as hydrogen (e^-p^+), positronium (e^-e^+), and muonium ($e^-\mu^+$) have long been recognized as the best tools to verify fundamental interaction theories (Kinoshita, 1990). This is because their energy levels can be calculated analytically or numerically to a high precision, limited in principle by the accuracy of fundamental physical constants. Starting with nonrelativistic quantum mechanics, the Hamiltonian of two charged particles with masses m_1 and m_2 interacting with an attractive Coulomb potential,

$$H = \frac{\vec{p}_1^2}{2m_1} + \frac{\vec{p}_2^2}{2m_2} - \frac{Z\alpha}{r} = E_k + H_0, \quad (1)$$

can be decomposed in terms of the total kinetic energy

$$E_k = \frac{(\vec{p}_1 + \vec{p}_2)^2}{2(m_1 + m_2)} \quad (2)$$

and the one-body Hamiltonian with the reduced mass μ

$$H_0 = \frac{\vec{p}^2}{2\mu} - \frac{Z\alpha}{r}, \quad (3)$$

where $\vec{p} = -i\vec{\nabla}_r$ is the relative momentum of these two particles. For a precise definition of constants and units, see Sec. II. The eigenvalues of this Hamiltonian

$$E_{nl} = -\frac{(Z\alpha)^2\mu}{2n^2} \quad (4)$$

depend on the principal quantum number $n = 1, 2, 3, \dots$ and not on the angular momentum number $l = 0, 1, \dots, n-1$. The degeneracy of states with different l is a characteristic feature of the nonrelativistic Coulomb Hamiltonian. We know, however, that a more accurate description of hydrogenlike levels must rely on the relativistic theory. The first questions arise here: What is the relativistic analog of the instantaneous Coulomb interaction, and what is the correct two-body equation for charged particles? In fact, there is no definitive answer to these questions yet. Only in the case in which the mass of one particle goes to infinity can we write a Dirac equation for the second spin-1/2 particle (or a Klein-Gordon equation for a spin-0 particle) in the Coulomb potential of a static nucleus (Itzykson and Zuber, 1980). For a hydrogen atom having a proton mass that is approximately 2000 times larger than the electron mass, the Dirac equation is a good starting point. It yields energy levels that depend not only on the principal quantum number n (as in the nonrelativistic case) but also on the total angular momentum number j , as well as on the fine structure constant α . Accordingly, the states $2S_{1/2}$ and $2P_{1/2}$ carry the same j and are thus degenerate. Here we use the historical notation, which is still used by atomic spectroscopists, where a state is labeled by its nL_j , with S, P, D, F, \dots standing for $l = 0, 1, 2, 3, \dots$, and the subscript j denoting the particular value of the total angular momentum.

However, in a true hydrogen atom the energy of the $2S_{1/2}$ state is slightly above that of the $2P_{1/2}$ one. This splitting, first observed experimentally by Lamb and Retherford (1947) and subsequently named the Lamb shift, was fundamental for the construction of quantum electrodynamics (QED) by Feynman, Schwinger, and Tomonaga, for which they were awarded the Nobel Prize (Dyson, 1965). QED theory allows us to account in a perturbative manner for the finite nuclear mass (Shabaev, 1998), for the electron self-interaction and the vacuum polarization (Itzykson and Zuber, 1980; Berestetskii, Lifshitz, and Pitaevskii, 1982), and, in current use, for the accurate description of not only hydrogenlike but also arbitrary atomic systems (Drake, 2023). All of these effects are described in Sec. III for such hydrogenlike systems, where the electron is replaced by the muon, a 200 times heavier lepton that is also a pointlike particle.

In contrast to leptons, however, the nucleus in most cases cannot be treated as a pointlike particle. For example, a proton has a finite charge distribution that can be measured in lepton-proton scattering experiments, as was first shown by Chambers and Hofstadter (1956). At present the nuclear charge distribution cannot be calculated *ab initio*, at least not with the accuracy needed by atomic spectroscopy measurements. This nuclear charge distribution affects the Coulomb interaction at small distances. Although it is a small effect (about 1 MHz in H), it needs to be taken into account due to the high accuracy of spectroscopic measurements; for example, the $1S-2S$ transition frequency in hydrogen (Parthey *et al.*, 2011) is

$$\nu_H(1S-2S) = 2466\,061\,413\,187\,035(10) \text{ Hz}. \quad (5)$$

The finite proton size effect can in principle be determined from the comparison of theoretical predictions for $\nu_H(1S-2S)$ to the aforementioned measurement. However, the Rydberg constant Ry enters into the comparison as a conversion constant between experiment (measured in SI units) and theory (performed in atomic units) (Pohl *et al.*, 2017; Tiesinga *et al.*, 2021). Thus far the only determination of Ry has been available from hydrogen itself because only this system can be calculated and measured accurately enough at the same time. Therefore, we need a second transition like $2S-nS$ to determine the two unknowns (Tiesinga *et al.*, 2021): the Rydberg constant and the mean square proton charge radius; see Eq. (73). Since the measurements of $2S-nS$ and other transitions in hydrogen are much less accurate, the atomic spectroscopy determination of the proton charge radius was of limited accuracy: $r_p = 0.8768(69)$ fm (Mohr, Taylor, and Newell, 2008), which is consistent with the electron-proton scattering determination (Bernauer *et al.*, 2014). This situation was stable for a long time, until a new determination of the proton charge radius became available from the Lamb shift measurement in muonic hydrogen μH (Pohl *et al.*, 2010). This new determination resulted in a much smaller proton charge radius of $r_p = 0.841\,84(67)$ fm and thus questioned the universality of electromagnetic interactions and the validity of QED theory for composite particles (Pohl *et al.*, 2013).

This is why the comparison of nuclear charge radii obtained at first from μH (Pohl *et al.*, 2010; Antognini *et al.*, 2013), then from μD (Pohl *et al.*, 2016), $\mu^4\text{He}$ (Krauth *et al.*, 2021), and $\mu^3\text{He}$ (Schuhmann *et al.*, 2023) to those obtained from “normal” atomic spectroscopy is a sensitive test of lepton universality and also a search for the existence of possible yet unknown lepton-nucleus interactions at the scale from a few to a few hundred femtometers; these interactions have not yet been probed experimentally by other means (Pohl *et al.*, 2013; Carlson, 2015). A similar or even stronger sensitivity to the lepton universality is expected from a direct comparison of the electron versus muon scattering of the proton, which is the aim of the MUSE Collaboration (Lorenzon, 2020). The charge radii of the proton and other light nuclei are also important for the determination of fundamental physical constants like the Rydberg constant from the spectroscopy of H (Tiesinga *et al.*, 2021) or He^+ (Herrmann *et al.*, 2009; Krauth *et al.*, 2020) and the electron-nucleus mass ratios from the spectroscopy of HD^+ (Alighanbari *et al.*, 2020; Patra *et al.*, 2020; Kortunov *et al.*, 2021). In fact, the global adjustment of fundamental constants, performed periodically every four years by CODATA (Tiesinga *et al.*, 2021), will now employ the nuclear charge radii obtained from muonic atom spectroscopy. Indeed, the most accurate determination of the root mean square (rms) nuclear charge radius r_C is by the measurement of the $2S - 2P$ transition in the hydrogenlike system, which consists of a muon and the nucleus (Pohl *et al.*, 2010; Antognini *et al.*, 2013). Owing to the 200-times-heavier muon, muonic atoms are much more sensitive to the nuclear size and to nuclear structure effects than normal electronic atoms. In particular, the rms radius shift of the muonic atom energy levels is $\sim 200^3$ larger than that of the electronic ones. Therefore, the determination of the nuclear charge radii from muonic atoms is much more accessible and precise. For this purpose, one needs to calculate QED and nuclear structure effects on the energy levels accurately enough to be able to interpret the remainder as a finite nuclear size effect. Borie and Rinker (1982) performed an extensive study of energy levels in muonic atoms by solving the Dirac equation with the muon mass replaced by the reduced mass of the muon-nucleus system, and by including the Breit interaction. This treatment partially accounts for the nuclear recoil corrections, but its results are not accurate enough for light muonic atoms. Therefore, an approach suited to light atomic systems, exact in the mass ratio, was developed by Pachucki (1996) and was widely followed in the later literature.

Here we present a comprehensive theory of the Lamb shift in light muonic atoms, with particular attention paid to the consistent separation of a point-nucleus QED from the nuclear structure effects. It is based mostly on the recent literature [see reviews by Antognini, Kottmann *et al.* (2013), Krauth *et al.* (2016), Franke *et al.* (2017), and Diepold *et al.* (2018) and references therein], with several contributions calculated or recalculated here. All results are shown in Table I, with each entry explained in its dedicated section. The crucial point is the preservation of consistency in the Lamb shift theory among all muonic and electronic atoms and, consequently, the consistent determination of nuclear charge radii.

II. EXPANSION OF ENERGY IN POWERS OF THE FINE STRUCTURE CONSTANT α

Throughout this review, we use the natural units $\hbar = c = 1$. We start with the definition of the Lamb shift in the presence of the nuclear spin \vec{I} , the spin of the orbiting lepton \vec{S} , and the angular momentum \vec{L} . The effective Hamiltonian in the subspace of states with a definite principal quantum number n , orbital momentum $l = 0$ or 1 , and nuclear spin $I \leq 1$ is

$$H_{\text{eff}}(n, l) = E_1 + E_2 \vec{S} \cdot \vec{L} + E_3 \vec{S} \cdot \vec{I} + E_4 \vec{L} \cdot \vec{I} + E_5 (L^i L^k)^{(2)} (I^i I^k)^{(2)} + E_6 (L^i L^k)^{(2)} I^i S^k, \quad (6)$$

where $(L^i L^k)^{(2)} = L^i L^k / 2 + L^k L^i / 2 - \vec{L}^2 \delta^{ik} / 3$. Here i and k are Cartesian indices; to distinguish them from Minkowski indices, the latter are denoted by lowercase greek letters. Furthermore, we use Einstein notation, which implies a sum over repeated indices. Note that we also limit the consideration to the case in which the orbiting lepton is a muon. Let $\vec{J} = \vec{L} + \vec{S}$; then for the $S_{1/2}$ state $l = 0$, $j = 1/2$, and we define $E(nS_{1/2}) = E_1(n, 0)$, while for the $P_{1/2}$ state

$$E(nP_{1/2}) = E_1(n, 1) + E_2(n, 1) \langle \vec{S} \cdot \vec{L} \rangle_{j=1/2} = E_1(n, 1) - E_2(n, 1), \quad (7)$$

so we calculate energies as if there were no nuclear spin couplings. Owing to the hyperfine mixing of the $P_{1/2}$ and $P_{3/2}$ states, this definition is not equivalent to the centroid energy but follows the definitions assumed in the literature devoted to muonic atoms and those of CODATA (Tiesinga *et al.*, 2021).

Having defined the Lamb shift

$$E_L = E(2P_{1/2}) - E(2S_{1/2}), \quad (8)$$

we employ an expansion in the fine structure constant $\alpha = e^2/4\pi$, with e the proton charge, to classify all important contributions and express E_L as the sum of many terms that have a definite power of α or $Z\alpha$ (where Z is the nuclear charge in units of e) but may depend on the muon-nucleus mass ratio in a nontrivial way. For this we assume that the electron vacuum polarization gives a single power of α (details are explained in Sec. III). All corrections up to α^5 are calculated with the exact mass dependence, while corrections of the order of α^6 are obtained using the expansion in the muon-nucleus mass ratio up to the linear term only because these higher-order corrections are almost negligible.

To obtain the numerical values in Table I, we use the following constants from the CODATA 2018 adjustment (Tiesinga *et al.*, 2021):

$$\alpha^{-1} = 137.035999084(21), \quad (9)$$

$$m_\mu = 105.6583755(23) \text{ MeV}, \quad (10)$$

$$\lambda_\mu = 1.867594306(42) \text{ fm}, \quad (11)$$

where m_μ is the mass and $\lambda_\mu = 1/m_\mu$ is the reduced Compton wavelength of the muon. The conversion constant that connects the energy and length units is

TABLE I. Contributions to the $2P_{1/2} - 2S_{1/2}$ energy difference E_L in meV, with the charge radii r_C given in fm. All corrections larger than 3% of the overall uncertainty are included. Theoretical predictions for E_L are $E_L(\text{theo}) = E_{\text{QED}} + Cr_C^2 + E_{\text{NS}}$. The last two rows show the values of r_C determined from a comparison of $E_L(\text{theo})$ to $E_L(\text{exp})$.

Section	Order	Correction	μH	μD	$\mu^3\text{He}^+$	$\mu^4\text{He}^+$
III.A	$\alpha(Z\alpha)^2$	eVP ⁽¹⁾	205.007 38	227.634 70	1641.886 2	1665.773 1
III.A	$\alpha^2(Z\alpha)^2$	eVP ⁽²⁾	1.658 85	1.838 04	13.084 3	13.276 9
III.A	$\alpha^3(Z\alpha)^2$	eVP ⁽³⁾	0.007 52	0.008 42(7)	0.073 0(30)	0.074 0(30)
III.B	$(Z, Z^2, Z^3)\alpha^5$	Light-by-light eVP	-0.000 89(2)	-0.000 96(2)	-0.013 4(6)	-0.013 6(6)
III.C	$(Z\alpha)^4$	Recoil	0.057 47	0.067 22	0.126 5	0.295 2
III.D	$\alpha(Z\alpha)^4$	Relativistic with eVP ⁽¹⁾	0.018 76	0.021 78	0.509 3	0.521 1
III.E	$\alpha^2(Z\alpha)^4$	Relativistic with eVP ⁽²⁾	0.000 17	0.000 20	0.005 6	0.005 7
III.F	$\alpha(Z\alpha)^4$	$\mu\text{SE}^{(1)} + \mu\text{VP}^{(1)}$, LO	-0.663 45	-0.769 43	-10.652 5	-10.926 0
III.G	$\alpha(Z\alpha)^5$	$\mu\text{SE}^{(1)} + \mu\text{VP}^{(1)}$, NLO	-0.004 43	-0.005 18	-0.174 9	-0.179 7
III.H	$\alpha^2(Z\alpha)^4$	$\mu\text{VP}^{(1)}$ with eVP ⁽¹⁾	0.000 13	0.000 15	0.003 8	0.003 9
III.I	$\alpha^2(Z\alpha)^4$	$\mu\text{SE}^{(1)}$ with eVP ⁽¹⁾	-0.002 54	-0.003 06	-0.062 7	-0.064 6
III.J	$(Z\alpha)^5$	Recoil	-0.044 97	-0.026 60	-0.558 1	-0.433 0
III.K	$\alpha(Z\alpha)^5$	Recoil with eVP ⁽¹⁾	0.000 14(14)	0.000 09(9)	0.004 9(49)	0.003 9(39)
III.L	$Z^2\alpha(Z\alpha)^4$	nSE ⁽¹⁾	-0.009 92	-0.003 10	-0.084 0	-0.050 5
III.M	$\alpha^2(Z\alpha)^4$	$\mu F_1^{(2)}, \mu F_2^{(2)}, \mu\text{VP}^{(2)}$	-0.001 58	-0.001 84	-0.031 1	-0.031 9
III.N	$(Z\alpha)^6$	Pure recoil	0.000 09	0.000 04	0.001 9	0.001 4
III.O	$\alpha(Z\alpha)^5$	Radiative recoil	0.000 22	0.000 13	0.002 9	0.002 3
III.P	$\alpha(Z\alpha)^4$	hVP	0.011 36(27)	0.013 28(32)	0.224 1(53)	0.230 3(54)
III.Q	$\alpha^2(Z\alpha)^4$	hVP with eVP ⁽¹⁾	0.000 09	0.000 10	0.002 6(1)	0.002 7(1)
IV.A	$(Z\alpha)^4$	r_C^2	-5.197 5 r_p^2	-6.073 2 r_d^2	-102.523 r_h^2	-105.322 r_α^2
IV.B	$\alpha(Z\alpha)^4$	eVP ⁽¹⁾ with r_C^2	-0.028 2 r_p^2	-0.034 0 r_d^2	-0.851 r_h^2	-0.878 r_α^2
IV.C	$\alpha^2(Z\alpha)^4$	eVP ⁽²⁾ with r_C^2	-0.000 2 r_p^2	-0.000 2 r_d^2	-0.009(1) r_h^2	-0.009(1) r_α^2
V.A	$(Z\alpha)^5$	TPE	0.029 2(25)	1.979(20)	16.38(31)	9.76(40)
V.B	$\alpha^2(Z\alpha)^4$	Coulomb distortion	0.0	-0.261	-1.010	-0.536
V.C	$(Z\alpha)^6$	3PE	-0.001 3(3)	0.002 2(9)	-0.214(214)	-0.165(165)
V.D	$\alpha(Z\alpha)^5$	eVP ⁽¹⁾ with TPE	0.000 6(1)	0.027 5(4)	0.266(24)	0.158(12)
V.E	$\alpha(Z\alpha)^5$	$\mu\text{SE}^{(1)} + \mu\text{VP}^{(1)}$ with TPE	0.000 4	0.002 6(3)	0.077(8)	0.059(6)
III	E_{QED}	Point nucleus	206.034 4(3)	228.774 0(3)	1644.348(8)	1668.491(7)
IV	Cr_C^2	Finite size	-5.225 9 r_p^2	-6.107 4 r_d^2	-103.383 r_h^2	-106.209 r_α^2
V	E_{NS}	Nuclear structure	0.028 9(25)	1.750 3(200)	15.499(378)	9.276(433)
	E_L (exp)	Experiment ^a	202.370 6(23)	202.878 5(34)	1258.598(48)	1378.521(48)
	r_C	This review	0.840 60(39)	2.127 58(78)	1.970 07(94)	1.678 6(12)
	r_C	Previous work ^a	0.840 87(39)	2.125 62(78)	1.970 07(94)	1.678 24(83)

^aPresented by Antognini *et al.* (2013), Pohl *et al.* (2016), Krauth *et al.* (2021), and Schuhmann *et al.* (2023).

$$\hbar c = 197.326\,980\,459\dots \text{MeV fm.} \quad (12)$$

The relevant mass ratios are

$$\frac{m_\mu}{m_e} = 206.768\,283\,0(46), \quad (13a)$$

$$\frac{m_\mu}{m_p} = 0.112\,609\,526\,4(25), \quad (13b)$$

$$\frac{m_\mu}{m_d} = 0.056\,332\,718\,3(13), \quad (13c)$$

$$\frac{m_\mu}{m_h} = 0.037\,622\,379\,7(8), \quad (13d)$$

$$\frac{m_\mu}{m_\alpha} = 0.028\,346\,557\,7(6), \quad (13e)$$

where the subscripts d , h , and α denote the deuteron, helion (^3He nucleus), and α particle (^4He nucleus),

respectively. Moreover, with μ the reduced mass of the two-body system,

$$\mu = \frac{m_\mu}{1 + m_\mu/M}, \quad (14)$$

with M standing for the nuclear mass, we define the ratio

$$\beta = \frac{m_e}{Z\alpha\mu}, \quad (15)$$

for which we obtain the following values:

$$\beta_p = 0.737\,383\,68, \quad (16a)$$

$$\beta_d = 0.700\,086\,14, \quad (16b)$$

$$\beta_h = 0.343\,842\,92, \quad (16c)$$

$$\beta_\alpha = 0.340\,769\,14. \quad (16d)$$

Finally, the nonrelativistic Coulomb wave function ϕ with nonrelativistic energy E_0 is the solution of $(H_0 - E_0)\phi = 0$, with H_0 as given by Eq. (3) and $E_0 = E_{nl}$ from Eq. (4). The radial parts of the wave function for the states of interest are

$$R_{20}(r) = \frac{(\mu Z \alpha)^{3/2}}{\sqrt{2}} \exp\left(-\frac{\mu Z \alpha r}{2}\right) \left(1 - \frac{\mu Z \alpha r}{2}\right), \quad (17)$$

$$R_{21}(r) = \frac{(\mu Z \alpha)^{3/2}}{2\sqrt{6}} \exp\left(-\frac{\mu Z \alpha r}{2}\right) \mu Z \alpha r, \quad (18)$$

and the wave function at the origin is

$$\phi_{nl}^2(0) = \frac{R_{nl}^2(0)}{4\pi} = \frac{(\mu Z \alpha)^3}{\pi n^3} \delta_{l0}. \quad (19)$$

Note that our choice of electromagnetic units is specified by the definition of α in terms of e . However, the expressions for the relevant energies [Eqs. (3) and (4)], the wave functions [Eqs. (17)–(19)], and the final results for the energy shifts do not depend on this choice. At the same time, intermediate quantities such as the photon propagator may change if one uses different electromagnetic units.

III. QED CONTRIBUTIONS TO THE LAMB SHIFT

To calculate QED corrections to the energy levels, we assume at first that the nucleus is pointlike, while the nuclear size and nuclear structure are considered separately in Secs. IV and V. A pointlike nucleus with spin 0 satisfies the Klein-Gordon equation, a nucleus with spin 1/2 satisfies the Dirac equation, and a nucleus with spin 1 satisfies the Proca equation, with the last corresponding to a g factor equal to 1. The radiative corrections on the nucleus line are included in the nuclear electromagnetic form factors and structure functions, with an exception described in Sec. III.L. As explained in Sec. II, all corrections up to $\alpha^5 m_\mu$ order are calculated with the exact muon-nuclear mass ratio, and $\alpha^6 m_\mu$ QED corrections are expanded in the mass ratio. We now start with the leading QED effects. Since we specialize in the case of an orbiting muon, from this point on we suppress the label on the muon mass, denoting it as m to make the equations more compact.

A. Electron vacuum polarization

The electron vacuum polarization (eVP) (see Fig. 1) modifies the photon propagator

$$-\frac{g^{\mu\nu}}{k^2} \rightarrow -\frac{g^{\mu\nu}}{k^2 [1 + \bar{\omega}(k^2/m_e^2)]}, \quad (20)$$

where $k^2 = (k^0)^2 - \vec{k}^2$ is the photon momentum squared. The sum of one-particle irreducible diagrams $\bar{\omega}$ is expanded in a power series of α/π ,

$$\bar{\omega} = \bar{\omega}^{(1)} + \bar{\omega}^{(2)} + \bar{\omega}^{(3)} + \dots, \quad (21)$$

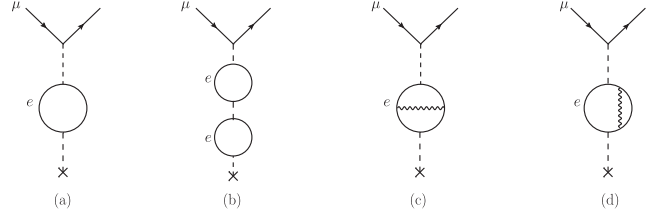


FIG. 1. Feynman diagrams for the pure QED electric vacuum polarization contribution to the Lamb shift. (a) Uehling potential. (b) Källén-Sabry potential, reducible two-loop part. (c), (d) Källén-Sabry potential, irreducible two-loop part.

which results in the following expansion of the photon propagator:

$$-\frac{g^{\mu\nu}}{k^2} \rightarrow -\frac{g^{\mu\nu}}{k^2} (1 + \rho^{(1)} + \rho^{(2)} + \rho^{(3)} + \dots), \quad (22)$$

where

$$\rho^{(1)} = -\bar{\omega}^{(1)}, \quad (23)$$

$$\rho^{(2)} = -\bar{\omega}^{(2)} + (\bar{\omega}^{(1)})^2, \quad (24)$$

$$\rho^{(3)} = -\bar{\omega}^{(3)} + 2\bar{\omega}^{(1)}\bar{\omega}^{(2)} - (\bar{\omega}^{(1)})^3. \quad (25)$$

Each $\rho^{(i)}$ generates an eVP potential $V^{(i)}(r)$ at $k^0 = 0$,

$$V^{(i)}(r) = -Z\alpha \int \frac{d^3k}{(2\pi)^3} \frac{4\pi}{\vec{k}^2} \rho^{(i)}(-\vec{k}^2) e^{i\vec{k}\cdot\vec{r}}, \quad (26)$$

and the corresponding corrections to the energy are

$$E^{(1)} = \langle V^{(1)} \rangle, \quad (27)$$

$$E^{(2)} = \langle V^{(2)} \rangle + \left\langle V^{(1)} \frac{1}{(E_0 - H_0)'} V^{(1)} \right\rangle, \quad (28)$$

$$E^{(3)} = \langle V^{(3)} \rangle + 2 \left\langle V^{(2)} \frac{1}{(E_0 - H_0)'} V^{(1)} \right\rangle + \left\langle V^{(1)} \frac{1}{(E_0 - H_0)'} (V^{(1)} - \langle V^{(1)} \rangle) \frac{1}{(E_0 - H_0)'} V^{(1)} \right\rangle, \quad (29)$$

where the prime in the denominator denotes a subtraction of the reference state. For example, at the one-loop level $V^{(1)}$ is

$$V^{(1)}(r) = -\frac{Z\alpha}{r} \frac{\alpha}{\pi} \int_4^\infty \frac{d(\xi^2)}{\xi^2} e^{-m_e \xi r} u(\xi^2), \quad (30)$$

where

$$u(\xi^2) = \frac{1}{3} \sqrt{1 - \frac{4}{\xi^2}} \left(1 + \frac{2}{\xi^2}\right), \quad (31)$$

and similarly

$$\bar{\omega}^{(1)}(\xi^2) = \frac{\alpha}{\pi} \xi^2 \int_4^\infty d(\xi'^2) \frac{1}{\xi'^2(\xi'^2 - \xi^2)} u(\xi'^2). \quad (32)$$

Using the radial functions for the $2P$ and $2S$ states from Eqs. (17) and (18), we find that the one-loop vacuum polarization contribution to the Lamb shift is

$$E_L^{(1)} = \mu(Z\alpha)^2 \frac{\alpha}{\pi} \int_4^\infty \frac{d(\xi^2)}{\xi^2} u(\xi^2) \frac{(\beta \xi)^2}{2(1 + \beta \xi)^4}, \quad (33)$$

with the numerical results presented in Table I. All of these one-, two-, and three-loop eVP contributions have already been obtained in the literature; see [Korzinin, Ivanov, and Karshenboim \(2013\)](#) and references therein. While the two-loop vacuum polarization (VP) is also known analytically ([Källén and Sabry, 1955](#)), the three-loop VP is known only numerically. It was first calculated for μH by [Kinoshita and Nio \(1999\)](#) and later corrected by [Ivanov, Korzinin, and Karshenboim \(2009\)](#) as well as by [Kinoshita and Nio \(2009\)](#). For other muonic atoms, [Korzinin, Ivanov, and Karshenboim \(2013\)](#) obtained approximate values, and the numerical values in Table I are taken from Table I of their work.

B. Light-by-light electron vacuum polarization

This contribution comes from a closed electron loop with four photon legs. These legs can be attached in all possible ways to the muon and the nucleus lines; see Fig. 2. There are three types of diagrams with one, two, or three legs attached to the muon and the remaining legs attached to the nucleus. Those with three legs attached to the nucleus are called the Wichmann-Kroll correction in the literature, those with two legs on each line are called the virtual Delbrück scattering correction, and those with one leg on the nucleus side we call here the inverted Wichmann-Kroll correction. They were all calculated by [Borie and Rinker \(1978\)](#), [Karshenboim *et al.* \(2010\)](#), and [Korzinin, Ivanov, and Karshenboim \(2013\)](#) (“LbL” in their Table I). The overall contribution is of the same order in α as the three-loop eVP but is about 10 times smaller.

C. Leading recoil $\sim (Z\alpha)^4$

This is the leading-order nuclear recoil contribution. The nonrelativistic energies of the $2S$ and $2P$ states are the same,

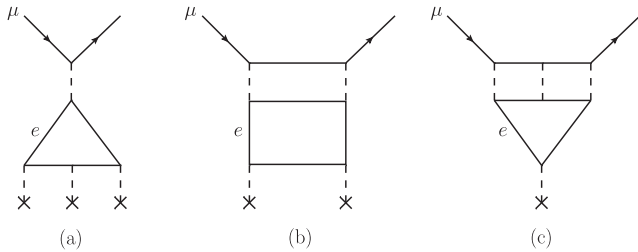


FIG. 2. Feynman diagrams for the light-by-light vacuum polarization contribution to the Lamb shift. (a) Wichmann-Kroll correction. (b) Virtual Delbrück scattering correction. (c) Inverted Wichmann-Kroll correction.

so the $(Z\alpha)^2$ recoil cancels out in the difference. The leading $(Z\alpha)^4$ relativistic correction is almost the same; the difference is quadratic in the muon-nucleus mass ratio. It is derived starting with the expectation value of the Breit-Pauli Hamiltonian $H^{(4)}$ ([Bethe and Salpeter, 1977](#)) with the non-relativistic wave function, namely,

$$\delta E = \langle H^{(4)} \rangle, \quad (34)$$

where

$$\begin{aligned} H^{(4)} = & -\frac{p^4}{8} \left(\frac{1}{m^3} + \frac{1}{M^3} \right) - \frac{Z\alpha}{2mM} p^i \left(\frac{\delta^{ij}}{r} + \frac{r^i r^j}{r^3} \right) p^j \\ & + \left(\frac{1}{4m^2} + \frac{1}{2mM} \right) \frac{Z\alpha}{r^3} \vec{r} \times \vec{p} \cdot \vec{\sigma} \\ & + \frac{\pi Z\alpha}{2} \left(\frac{1}{m^2} + \frac{\delta_I}{M^2} + \frac{4}{3} r_C^2 \right) \delta^{(3)}(\vec{r}), \end{aligned} \quad (35)$$

and where $\delta_I = 1$ for $I = 1/2$, and $\delta_I = 0$ for $I = 0$ and 1 by convention ([Pachucki and Karshenboim, 1995](#)). This results from the assumption that the scalar particle satisfies the Klein-Gordon equation and the vector particle satisfies the Proca equation. The Hamiltonian (35) includes the finite nuclear size correction, the treatment of which is deferred to Sec. IV; see Eq. (72). Without the finite size term, Eq. (35) yields for the $2P_{1/2} - 2S_{1/2}$ energy difference ([Jentschura, 2011b](#))

$$\delta E_L = \begin{cases} (Z\alpha)^4 \mu^3 / (48 M^2) & \text{for } \delta_I = 1, \\ (Z\alpha)^4 \mu^3 / (12 M^2) & \text{for } \delta_I = 0, \end{cases} \quad (36)$$

with the numerical results presented in Table I.

D. Relativistic correction with the one-loop electron vacuum polarization

This is a contribution of the order of $\alpha(Z\alpha)^4$ that combines the leading relativistic corrections with the one-loop eVP. To derive it, we construct the photon propagator $G^{\mu\nu}$ in the modified Coulomb gauge. What we mean is the following: We require the time component G^{00} of the propagator to coincide with the Coulomb potential including the vacuum polarization charge density, namely, $G^{00} = \rho(\vec{k}^2)/\vec{k}^2$. The transverse part of the propagator has to be of the form ([Pachucki and Yerokhin, 2023](#))

$$G^{ij}(k) = \frac{\rho(-k^2)}{k^2} \left(\delta^{ij} - \frac{k^i k^j}{(k^0)^2} \right) - \frac{k^i k^j}{(k^0)^2} \frac{\rho(\vec{k}^2)}{\vec{k}^2} \quad (37)$$

in order to be equivalent to the well-known propagator in the Feynman gauge

$$G_F^{\mu\sigma}(k) = -\frac{g^{\mu\sigma}}{k^2} \rho(-k^2). \quad (38)$$

For the evaluation of relativistic corrections with eVP, one needs the coordinate-space representation of the propagator at $k^0 = 0$, which is

$$G^{00}(\vec{r}) = \int \frac{d^3k}{(2\pi)^3} e^{i\vec{k}\cdot\vec{r}} \frac{\rho(\vec{k}^2)}{k^2}, \quad (39)$$

$$G^{ij}(\vec{r}) = -\frac{1}{2} \left(\delta^{ij} - \frac{r^i r^j}{r} \frac{d}{dr} \right) G^{00}(\vec{r}). \quad (40)$$

In the case of $\rho(\vec{k}^2) = 1$ it becomes

$$G^{00}(\vec{r}) = \frac{1}{4\pi r}, \quad (41)$$

$$G^{ij}(\vec{r}) = -\frac{1}{8\pi} \left(\frac{\delta^{ij}}{r} + \frac{r^i r^j}{r^3} \right), \quad (42)$$

the standard Coulomb gauge propagator at $k^0 = 0$. One can now repeat the derivation of the Breit-Pauli Hamiltonian $H^{(4)}(V)$, as done by Veitia and Pachucki (2004), using the aforementioned modified Coulomb propagator,

$$\begin{aligned} H^{(4)}(V) = & -\frac{p^4}{8} \left(\frac{1}{m^3} + \frac{1}{M^3} \right) + \frac{1}{8} \left(\frac{1}{m^2} + \frac{\delta_l}{M^2} \right) \nabla^2 V \\ & + \left(\frac{1}{4m^2} + \frac{1}{2mM} \right) \frac{V'}{r} \vec{L} \cdot \vec{\sigma} \\ & + \frac{1}{2mM} \left[\nabla^2 \left(V - \frac{1}{4}(rV)' \right) + \frac{V'}{r} \vec{L}^2 \right. \\ & \left. + \frac{p^2}{2} (V - rV') + (V - rV') \frac{p^2}{2} \right], \end{aligned} \quad (43)$$

and obtain the correction

$$\delta E = \langle H^{(4)}(V^{(1)}) \rangle + 2 \left\langle V^{(1)} \frac{1}{(E_0 - H_0)'} H^{(4)} \right\rangle, \quad (44)$$

where $H^{(4)} = H^{(4)}(-Z\alpha/r)$. Equation (44) was first derived and calculated for μH by Pachucki (1996), but with some mistakes. We take the numerical values from Table I of Jentschura (2011b), who corrected these mistakes and calculated Eq. (44) for all nuclei of interest. The use of $G^{ij}(\vec{r})$ from Eq. (40) will allow for future nonperturbative calculations of eVP corrections by solving the Schrödinger or Dirac equation numerically, which is much more efficient for heavier elements.

E. Relativistic correction with the two-loop electron vacuum polarization

This correction is of the order of $\alpha^2(Z\alpha)^4$ and can be obtained as in the one-loop case in Sec. III.D. However, Korzinin, Ivanov, and Karshenboim (2013) calculated it numerically using a slightly different approach that employed the Dirac equation. The numerical values (see their Table VI) are about 1% of the one-loop case and are shown in Table I.

F. Leading muon self-energy and vacuum polarization

For the calculation of the one-loop muon self-energy $\mu\text{SE}^{(1)}$ and the muon vacuum polarization $\mu\text{VP}^{(1)}$ corrections to the Lamb shift, we rewrite the corresponding formula known for electronic hydrogen,

$$\begin{aligned} E(2S_{1/2}) = & \frac{1}{8} m \frac{\alpha}{\pi} (Z\alpha)^4 \left(\frac{\mu}{m} \right)^3 \left[\frac{10}{9} - \frac{4}{15} - \frac{4}{3} \ln k_0(2S) \right. \\ & \left. + \frac{4}{3} \ln \left(\frac{m}{\mu(Z\alpha)^2} \right) \right], \end{aligned} \quad (45)$$

$$E(2P_{1/2}) = \frac{1}{8} m \frac{\alpha}{\pi} (Z\alpha)^4 \left(\frac{\mu}{m} \right)^3 \left[-\frac{1}{6} \frac{m}{\mu} - \frac{4}{3} \ln k_0(2P) \right], \quad (46)$$

where $\ln k_0(n, l)$ is the Bethe logarithm,

$$\ln k_0(2S) = 2.811\,769\,893\,1\dots, \quad (47)$$

$$\ln k_0(2P) = -0.030\,016\,708\,9\dots, \quad (48)$$

which is the same for electronic and for muonic hydrogen-like atoms.

G. Next-to-leading muon self-energy and vacuum polarization

This is a two-photon exchange contribution accompanied by the one-loop self-energy $\mu\text{SE}^{(1)}$ or vacuum polarization $\mu\text{VP}^{(1)}$. For a point nucleus it is given by a contact interaction and thus has the same form for electronic and muonic hydrogenlike atoms, namely (Eides, Grotch, and Shelyuto, 2001),

$$\delta E(n, l) = \frac{\alpha(Z\alpha)^5}{\pi n^3} \frac{\mu^3}{m^2} 4\pi \left(\frac{139}{128} + \frac{5}{192} - \frac{\ln 2}{2} \right) \delta_{l0}, \quad (49)$$

where the second term in parentheses comes from $\mu\text{VP}^{(1)}$. There is a nuclear recoil correction to this formula that is considered in Sec. III.O, and there is also a finite nuclear size correction that is considered in Sec. V.E.

H. Combined muon and electron vacuum polarizations

Correction to the energy due to $\mu\text{VP}^{(1)}$ can be represented as a contact interaction,

$$\delta E = -\frac{4}{15m^2} \alpha(Z\alpha) \langle \delta^{(3)}(r) \rangle = -\frac{1}{15m^2} \frac{\alpha}{\pi} \langle \nabla^2 V \rangle, \quad (50)$$

where $V = -Z\alpha/r$. Combining this contact interaction with the perturbation due to $\text{eVP}^{(1)}$, one obtains

$$\delta E = -\frac{2}{15m^2} \frac{\alpha}{\pi} [\langle \nabla^2 V^{(1)} \rangle + 4\pi Z\alpha \phi(0) \delta\phi(0)], \quad (51)$$

where

$$|\delta\phi\rangle = \frac{1}{(E_0 - H_0)'} V^{(1)} |\phi\rangle. \quad (52)$$

This correction was obtained by Eides, Grotch, and Shelyuto (2001), among many others. Particular values for the considered muonic atoms were taken from Korzinin, Ivanov, and Karshenboim (2013).

I. Muon self-energy combined with the electron vacuum polarization

This is similar to the previous correction, with $\mu\text{VP}^{(1)}$ replaced by $\mu\text{SE}^{(1)}$. It is the one-loop muon self-energy in the Coulomb potential with one $\text{eVP}^{(1)}$ insertion. For its derivation we generalize Eqs. (45) and (46) to an arbitrary potential

$$\begin{aligned} \delta E = & \frac{\alpha}{4\pi m^2} \langle \phi | \nabla^2(V) | \phi \rangle \left[\frac{10}{9} + \frac{4}{3} \ln \left(\frac{m}{\mu(Z\alpha)^2} \right) \right] \\ & + \frac{2\alpha}{3\pi m^2} \langle \phi | \vec{\nabla} (H - E) \ln \left(\frac{2(H - E)}{\mu(Z\alpha)^2} \right) \vec{\nabla} | \phi \rangle \\ & + \frac{\alpha}{4\pi m \mu} \langle \phi | \frac{V'}{r} \vec{L} \cdot \vec{\sigma} | \phi \rangle, \end{aligned} \quad (53)$$

where H is the nonrelativistic Hamiltonian with the potential V and eigenenergy E . The perturbation due to $V^{(1)}$ was first estimated by Pachucki (1996). The complete calculation including the perturbed Bethe logarithm was performed by Jentschura and Wundt (2011) in their Eqs. (29a)–(29d), and in Table I we use their results.

J. Recoil $\sim (Z\alpha)^5$

This is the $(Z\alpha)^5$ contribution to the energy of two bound point particles, the muon and the nucleus, without any radiative corrections. It vanishes in the limit of a heavy nucleus; therefore, we call it a recoil correction. It depends not only on the muon-nucleus mass ratio but also on the value of the nuclear spin I . The explicit formula was derived originally for the spin $I = 1/2$ nucleus by Salpeter (1952) and Erickson (1977); this formula was valid for an arbitrary mass ratio. Here we extend this formula to the case in which one of the particles has spin $I = 0$ or 1 using derivations presented in Sec. V.A. The result is

$$\begin{aligned} E(n, l) = & \frac{\mu^3}{mM} \frac{(Z\alpha)^5}{\pi n^3} \left\{ \frac{2}{3} \delta_{l0} \ln \left(\frac{1}{Z\alpha} \right) - \frac{8}{3} \ln k_0(n, l) \right. \\ & - \frac{1}{9} \delta_{l0} - \frac{7}{3} a_n - 2 \delta_{l0} \ln \left(1 + \frac{m}{M} \right) \\ & \left. + \frac{m^2}{M^2 - m^2} \ln \left(\frac{M}{m} \right) \delta_{l0} [2 + I(2I - 1)] \right\}, \end{aligned} \quad (54)$$

where

$$\begin{aligned} a_n = & -2 \left[\ln \left(\frac{2}{n} \right) + \left(1 + \frac{1}{2} + \dots + \frac{1}{n} \right) + 1 - \frac{1}{2n} \right] \delta_{l0} \\ & + \frac{1 - \delta_{l0}}{l(l+1)(2l+1)}. \end{aligned} \quad (55)$$

It agrees with that of Shelyuto, Korzinin, and Karshenboim (2018, 2019) for $I = 0$ and 1 nuclei under the assumption that

$g = 1$. For other values of g , this recoil correction would have a logarithmic UV divergence. Numerical results using Eq. (54) for all nuclei are shown in Table I.

K. Recoil with the electron vacuum polarization

This is the $\text{eVP}^{(1)}$ correction to the $(Z\alpha)^5$ contribution in Eq. (54). It is difficult to calculate; in fact, it was obtained only by Jentschura and Wundt (2011) and only in the logarithmic approximation. The results shown in Table I are numerically small and suppressed with respect to the leading recoil correction given in Eq. (54) by a factor of α . To account for nonlogarithmic terms, we assume a conservative 100% uncertainty.

L. Nuclear self-energy

If we assume a pointlike nucleus with spin 1/2, the contribution of the nuclear self-energy for an arbitrary hydrogenic state is

$$E(n, l) = \frac{Z(Z\alpha)^5 \mu^3}{\pi n^3 M^2} \left[\left(\frac{10}{9} + \frac{4}{3} \ln \frac{M}{\mu(Z\alpha)^2} \right) \delta_{l0} - \frac{4}{3} \ln k_0(n, l) \right]. \quad (56)$$

For a nonpointlike nucleus there is a finite size correction. The problem is that the nuclear self-energy is modified by, and modifies as well, the finite size effect. To incorporate the correction (56) unambiguously, we must precisely specify the nuclear mean square charge radius. The usual definition through the Sachs electric form factor

$$\frac{r_C^2}{6} = \left. \frac{\partial G_E(q^2)}{\partial(q^2)} \right|_{q^2=0} \quad (57)$$

is not correct at our precision level, because G_E cannot be uniquely defined in the presence of electromagnetic interactions. Following Pachucki (1995) we propose a different definition using the forward scattering amplitude described by

$$T^{\mu\nu}(q) = -i \int d^4x e^{iqx} \langle t | T j^\mu(x) j^\nu(0) | t \rangle, \quad (58)$$

where $t = (M, 0, 0, 0)$. We consider the behavior of the dominant T^{00} component at small q^2 and $p^2 - M^2 = (t+q)^2 - M^2$. For a pointlike particle without self-energy corrections, one finds that

$$\begin{aligned} T^{00} = & \text{Tr} \left[\gamma^0 \frac{1}{\not{p} - M} \gamma^0 \frac{(\gamma^0 + I)}{4} \right] + (q \rightarrow -q) \\ \approx & \frac{2M}{p^2 - M^2} + (q \rightarrow -q). \end{aligned} \quad (59)$$

For a finite size particle without self-energy corrections

$$\gamma^\mu \rightarrow \Gamma^\mu = \gamma^\mu F_1(q^2) + i \frac{\sigma^{\mu\nu}}{2M} q_\nu F_2(q^2), \quad (60)$$

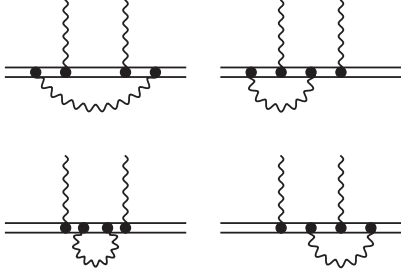


FIG. 3. Feynman diagrams for the radiative corrections to the forward Compton scattering off a nucleus.

T^{00} acquires a correction

$$\begin{aligned} \Delta T^{00} &\approx \frac{2M}{p^2 - M^2} [G_E^2(q^2) - 1] + (q \rightarrow -q) \\ &\approx \frac{2M}{p^2 - M^2} q^2 \frac{r_C^2}{3} + (q \rightarrow -q), \end{aligned} \quad (61)$$

where $G_E = F_1 + (q^2/4M^2)F_2$. The self-energy corrections for a pointlike particle coming from the diagrams in Fig. 3 are (Pachucki, 1995)

$$\Delta T^{00} = \frac{Z^2 \alpha}{\pi M} \frac{q^2}{p^2 - M^2} \left(\frac{10}{9} + \frac{4}{3} \ln \frac{M^2}{M^2 - p^2} \right) + (q \rightarrow -q). \quad (62)$$

We thus define r_C^2 using the following equation, which describes the low-energy behavior of the correction to the forward scattering amplitude of a pointlike particle:

$$\Delta T^{00} = \frac{q^2 M}{p^2 - M^2} \left(\frac{4Z^2 \alpha}{3\pi M^2} \ln \frac{M^2}{M^2 - p^2} + \frac{2}{3} r_C^2 \right) + (q \rightarrow -q). \quad (63)$$

We expect that for any nucleus the aforementioned logarithmic term will be the same because it is related only to the fact that the nucleus has a charge; it does not depend on other details like its spin. There is an arbitrariness in the choice of the constant term, i.e., what belongs to the charge radius and what belongs to the nuclear self-energy. The proposed definition separates only the logarithmic term from the charge radius; thus, the associated correction to the energy has the form

$$\begin{aligned} E(n, l) &= \frac{2}{3n^3} (Z\alpha)^4 \mu^3 r_C^2 \delta_{l0} \\ &+ \frac{4Z(Z\alpha)^5 \mu^3}{3\pi n^3 M^2} \left[\ln \left(\frac{M}{\mu(Z\alpha)^2} \right) \delta_{l0} - \ln k_0(n, l) \right], \end{aligned} \quad (64)$$

where the correction for P states beyond $\ln k_0(n, l)$ goes into the nuclear magnetic moment. The same formula for the nuclear self-energy will be assumed for all nuclei, and numerical results coming from the second line of Eq. (64) are presented in Table I.

M. Muon two-loop form factors and vacuum polarization

This correction comes from the muon two-loop form factors and the two-loop vacuum polarization $\mu\text{VP}^{(2)}$:

$$E(nS_{1/2}) = \frac{\mu^3}{m^2} \left(\frac{\alpha}{\pi} \right)^2 \frac{(Z\alpha)^4}{n^3} \left(4F_1'(0) + F_2(0) - \frac{82}{81} \right), \quad (65)$$

$$E(nP_{1/2}) = \frac{\mu^2}{m} \left(\frac{\alpha}{\pi} \right)^2 \frac{(Z\alpha)^4}{n^3} \left(-\frac{1}{3} \right) F_2(0), \quad (66)$$

where the muon two-loop form factors are (Barbieri, Caffo, and Remiddi, 1973)

$$\begin{aligned} F_1'(0) &= -\frac{3\zeta(3)}{4} - \frac{4819}{5184} - \frac{49\pi^2}{432} + \frac{1}{2}\pi^2 \ln 2 \\ &+ \left[\frac{1}{9} \ln^2 \frac{m}{m_e} - \frac{29}{108} \ln \frac{m}{m_e} + \frac{\pi^2}{54} + \frac{395}{1296} + O\left(\frac{m_e}{m}\right) \right] \end{aligned} \quad (67)$$

and

$$\begin{aligned} F_2(0) &= \frac{3\zeta(3)}{4} + \frac{197}{144} + \frac{\pi^2}{12} - \frac{1}{2}\pi^2 \ln 2 \\ &+ \left[\frac{1}{3} \ln \frac{m}{m_e} - \frac{25}{36} + O\left(\frac{m_e}{m}\right) \right]. \end{aligned} \quad (68)$$

The terms in square brackets in Eqs. (67) and (68) come from the closed electron loop and thus are dominant. Numerical results for all muonic atoms of interest are presented in Table I.

N. Pure recoil $\sim (Z\alpha)^6$

The $(Z\alpha)^6$ contribution to the energy of a bound system of two particles is expanded in the mass ratio m/M . The nonrecoil term coincides with the Dirac energy and thus vanishes in the $2P_{1/2} - 2S_{1/2}$ difference. The leading term is linear in the mass ratio and is given by (Pachucki and Grotch, 1995; Jentschura and Pachucki, 1996)

$$\delta E_L = -\frac{m^2 (Z\alpha)^6}{M} \left(\frac{1}{3} + 4 \ln 2 - \frac{7}{2} \right), \quad (69)$$

which results in a relatively small correction; see Table I.

O. Radiative recoil $\sim \alpha(Z\alpha)^5$

The $\alpha(Z\alpha)^5$ contribution to the energy is given by a contact interaction and is thus proportional to $\phi^2(0)$. We expand the coefficient in powers of the muon-nucleus mass ratio m/M . The nonrecoil term was already accounted for in Sec. III.G; the next term in the mass ratio expansion is the radiative recoil correction (Pachucki, 1995; Eides, Grotch, and Shelyuto, 2001),

$$\delta E_L = \frac{\mu^3}{mM} \frac{\alpha(Z\alpha)^5}{8} 1.36449, \quad (70)$$

which includes $\mu\text{SE}^{(1)}$ and $\mu\text{VP}^{(1)}$.

P. Hadronic vacuum polarization

To estimate the effect of the hadronic vacuum polarization (hVP), we assume “the most realistic value” according to Karshenboim and Shelyuto (2021) (“Scatter” in their Table 4).

Using as a reference the energy shift due to $\mu\text{VP}^{(1)}$ [the second term in Eq. (45)], we write the hVP contribution as

$$E(n, l) = \frac{\mu^3}{m^2} \frac{\alpha (Z\alpha)^4}{\pi n^3} \left(-\frac{4}{15} \right) \gamma_{\text{had}} \delta_{l0}. \quad (71)$$

Equation (71) differs from the $\mu\text{VP}^{(1)}$ term by a factor of $\gamma_{\text{had}} = 0.6746(160)$, thus giving an appreciable effect that should be included in the same way in muonic and electronic atoms to obtain consistent nuclear charge radii. The corresponding numerical values are shown in Table I.

Q. Combined electron and hadronic vacuum polarization

We represent this correction as the aforementioned coefficient γ_{had} times the correction due to $\mu\text{VP}^{(1)}$ combined with $\text{eVP}^{(1)}$ from Sec. III.H.

IV. FINITE NUCLEAR SIZE CONTRIBUTION

All corrections in this section are proportional to the mean square charge radius and thus have the form $C r_C^2$.

A. Leading finite size r_C^2

The definition of the rms charge radius r_C^2 depends on the nuclear spin and, in particular, there are different definitions for a spin-1 particle, such as the deuteron, as discussed by Jentschura (2011a). For a particle with spin I and mass M , r_C^2 can be defined through the effective interaction with the electromagnetic field,

$$\delta H = e A^0 - e \left(\frac{r_C^2}{6} + \frac{\delta_I}{8M^2} \right) \vec{\nabla} \cdot \vec{E} - \frac{e}{2I(2I-1)} (I^i I^j)^{(2)} \nabla^j E^i - \frac{\mu_I}{I} \vec{I} \cdot \vec{B}, \quad (72)$$

where μ_I and Q are the magnetic dipole and electric quadrupole moments, and the Darwin-Foldy term δ_I has been defined after Eq. (35). Namely, for a scalar particle $\delta_0 = 0$, and for a spin-1/2 particle the Dirac equation gives $\delta_{1/2} = 1$. For a vector particle, we assume that the charge radius is defined with respect to the Proca particle, namely, the point vector particle with $g = 1$ and $Q = 0$, and this gives $\delta_1 = 0$ (Pachucki and Karshenboim, 1995). This convention coincides with the definition employed in nuclear physics (Filin *et al.*, 2021) and affects the relativistic recoil correction (see Sec. III.C), while the finite nuclear size correction is

$$E_{\text{FNS}}(n, l) = \frac{2\pi}{3} Z \alpha \phi^2(0) r_C^2 = \frac{2}{3n^3} (Z\alpha)^4 \mu^3 r_C^2 \delta_{l0}. \quad (73)$$

Apart from the spin dependence, the nuclear self-energy affects the definition of r_C . This is described in Sec. III.L, where following Pachucki (1995) we propose using the forward two-photon exchange amplitude for the precise definition of the nuclear charge radius.

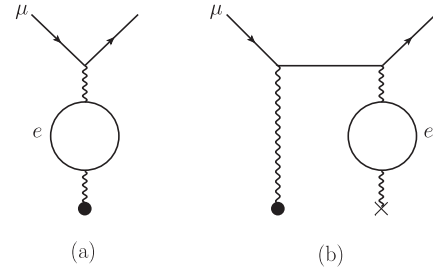


FIG. 4. One-loop electron vacuum polarization corrections to the nuclear finite size. (a) Photon propagator correction. (b) Wave function correction.

B. One-loop electron vacuum polarization with r_C^2

The leading QED correction to the finite size contribution is due to the one-loop eVP and is described by two terms (Pachucki, 1996), corresponding to the two diagrams in Fig. 4,

$$\delta E_{\text{FNS}} = \frac{r_C^2}{6} [\langle \nabla^2 V^{(1)} \rangle + 8\pi Z \alpha \phi(0) \delta \phi(0)]. \quad (74)$$

The correction is proportional to r_C^2 , and the coefficient is presented in Table I.

C. Two-loop electron vacuum polarization with r_C^2

This is a correction similar to the previous one but is suppressed by an additional factor of α . Thus, it is almost negligible. It was calculated by Martynenko, Krutov, and Shamsutdinov (2014) for μD in their Eqs. (30)–(32), and by Krutov *et al.* (2015) for μHe^+ (items 18 and 19 in their Table I). Because they neglected third-order perturbation theory diagrams, we have added a conservative uncertainty of 10% to their results. Finally, the result for μH was obtained by rescaling it from μD .

V. NUCLEAR STRUCTURE CONTRIBUTIONS

The nuclear structure contributions beyond the finite nuclear size are expanded in powers of the fine structure constant α , as with all other corrections. We call the leading term of the order of $(Z\alpha)^5$ the two-photon exchange (TPE). There are several corrections of higher order in α , which are all considered in separate sections. Moreover, we assume that the possible radiative corrections on the nucleus line are all included in E_{TPE} , with the exception of the leading nuclear self-energy considered in Sec. III.L.

A. Two-photon exchange

The $(Z\alpha)^5$ TPE contribution in a muonic atom with a nucleus of spin I is given by (Pachucki, 1999)

$$\begin{aligned} E_{\text{TPE}} &= -\frac{(Ze^2)^2}{2} \phi^2(0) \int_s \frac{d^4 q}{(2\pi)^4 i} \frac{1}{q^4} [T^{\mu\nu} - t^{\mu\nu}(I, M)] t_{\mu\nu}(m) \\ &= -2(Ze^2)^2 \phi^2(0) \frac{m}{M} \int_s \frac{d^4 q}{(2\pi)^4 i} \\ &\quad \times \frac{[T_2 - t_2(I, M)](q^2 - \nu^2) - [T_1 - t_1(I, M)](q^2 + 2\nu^2)}{q^4(q^4 - 4m^2\nu^2)}, \end{aligned} \quad (75)$$

where $T^{\mu\nu}$ is the forward virtual Compton scattering amplitude, defined in Eq. (58), that can be expressed in terms of two Lorentz invariant functions $T_1(\nu, -q^2)$ and $T_2(\nu, -q^2)$,

$$T^{\mu\nu} = -\left(g^{\mu\nu} - \frac{q^\mu q^\nu}{q^2}\right) \frac{T_1}{M} + \left(\frac{t^\mu}{M} - \frac{\nu}{q^2} q^\mu\right) \left(\frac{t^\nu}{M} - \frac{\nu}{q^2} q^\nu\right) \frac{T_2}{M}, \quad (76)$$

and where $\nu = q^0$ is the lab-frame photon energy. To be consistent with the $(Z\alpha)^5$ recoil correction in Eq. (54), we assume in Eq. (75) that $t^{\mu\nu}(I, M)$ corresponds to the pointlike nucleus of spin I . For $I = 1/2$, $t^{\mu\nu}(M) \equiv t^{\mu\nu}(1/2, M)$, and

$$t^{\mu\nu}(M) = \text{Tr} \left[\gamma^\mu \frac{1}{\not{p} - M} \gamma^\nu \frac{\not{p}^0 + I}{4} \right] + (q \rightarrow -q), \quad (77)$$

with $p = t + q$. From Eq. (77) one obtains for a point Dirac particle

$$t_1(1/2, M) = -\frac{4M^2\nu^2}{q^4 - 4M^2\nu^2}, \quad (78)$$

$$t_2(1/2, M) = \frac{4M^2q^2}{q^4 - 4M^2\nu^2}. \quad (79)$$

For a point scalar particle one obtains

$$t_1(0, M) = 1, \quad (80)$$

$$t_2(0, M) = \frac{4M^2q^2}{q^4 - 4M^2\nu^2}, \quad (81)$$

and for a Proca vector particle (Lee and Yang, 1962)

$$t_1(1, M) = -\frac{2\nu^2(6M^2 - q^2) - q^4}{3(q^4 - 4M^2\nu^2)}, \quad (82)$$

$$t_2(1, M) = \frac{2q^2(6M^2 - q^2)}{3(q^4 - 4M^2\nu^2)}. \quad (83)$$

The subscript s in the integral in Eq. (75) denotes an additional subtraction of a $1/q^5$ singularity, which has to be proportional to r_C^2 provided the subtraction of a point nucleus with an appropriate spin is assumed.

We now make a digression regarding the pure recoil $(Z\alpha)^5$ correction. It was originally calculated for the point spin-1/2 nucleus. The difference between an arbitrary spin I and a spin-1/2 point nuclei of the same mass is given by

$$\delta E = -2(Ze^2)^2 \phi^2(0) \frac{m}{M} \int_s \frac{d^4q}{(2\pi)^4 i} \times \frac{[t_2(I) - t_2(1/2)](q^2 - \nu^2) - [t_1(I) - t_1(1/2)](q^2 + 2\nu^2)}{q^4(q^4 - 4m^2\nu^2)}, \quad (84)$$

using the aforementioned $t_{1,2}$ functions with the mass argument implicit. This δE gives the term proportional to $I(2I - 1)$ in Eq. (54), which generalizes the pure recoil correction to the case of spin $I = 0, 1$ point nuclei, while for higher spins this integral diverges.

We now make a second digression. $T^{\mu\nu}$ is a complete forward virtual Compton scattering amplitude and thus includes radiative corrections. Consequently, it has a $\ln(M^2 - p^2)$ singularity at the threshold; see Eq. (63) with $p = t + q$ and $t = (M, \vec{0})$. This singularity comes from the nuclear self-energy, and thus the corresponding $\ln q/q^5$ singularity should also be subtracted out in Eq. (84). The last subtraction is not mentioned in any calculation of the TPE correction from the scattering amplitudes, but it should because $T^{\mu\nu}$ on the nucleus line is a complete amplitude. Moreover, the presence of the logarithmic singularity at threshold indicates the lack of the possibility to separate $T^{\mu\nu}$ into elastic and inelastic contributions. However, we neglect this singularity and disregard the associated difficulties in what follows because the related effect is negligible at the current precision level.

1. TPE in μH

Returning to the calculation of TPE in Eq. (75), we find that it is conventionally split into a Born and a polarizability part,

$$E_{\text{TPE}}(\mu\text{H}) = E_{\text{Born}} + E_{\text{pol}}. \quad (85)$$

The Born contribution

$$E_{\text{Born}} = E_{\text{Fri}} + E_{\text{rec}} \quad (86)$$

in the infinite nuclear mass limit is given by

$$E_{\text{Fri}} = -\frac{\pi}{3} \phi^2(0) (Z\alpha)^2 \mu r_F^3, \quad (87)$$

where r_F is the Friar radius

$$r_F^3 = \int d^3r_1 \int d^3r_2 \rho(r_1) \rho(r_2) |\vec{r}_1 - \vec{r}_2|^3, \quad (88)$$

and the remainder is given by the small recoil correction E_{rec} . The presence of μ instead of m in Eq. (87) is a matter of convention, and this affects the definition of the TPE recoil correction. For the polarizability part

$$E_{\text{pol}} = E_{\text{sub}} + E_{\text{inel}}, \quad (89)$$

one can use dispersion relations to express T_1 and T_2 in terms of proton structure functions measured in electron-proton scattering. In the case of T_1 , a once-subtracted dispersion relation is needed, giving rise to the subtraction function $T_1(0, -q^2)$, which cannot be measured directly, but has to be modeled or predicted from chiral perturbation theory (χPT), covariant (Alarcon, Lensky, and Pascalutsa, 2014; Lensky *et al.*, 2018), or heavy baryon (Birse and McGovern, 2012; Peset and Pineda, 2014, 2015a, 2015b). The inelastic structure functions needed for the dispersive evaluation are known only

for the proton, deuteron, and helion, although not in the entire kinematic region, especially for the deuteron and helion; thus, a different approach will have to be employed for nuclei other than the proton.

In the case of the $2S$ state of μH , the Friar contribution

$$E_{\text{Fri}} = -0.0211(2) \text{ meV} \quad (90)$$

is obtained using the recent Friar radius $r_{\text{F}}^3(p) = 2.310(26) \text{ fm}^3$ from Lin, Hammer, and Meißner (2022). Their work is a dispersive fit of nucleon form factors based on data in both the spacelike and timelike regions. Note that the dispersive analyses of the proton form factor (Mergell, Meißner, and Drechsel, 1996; Belushkin, Hammer, and Meißner, 2007; Lorenz *et al.*, 2015) predicted the smaller proton charge radius $r_p = 0.84 \text{ fm}$ before the μH Lamb shift measurement. These analyses have improved since then, taking into consideration new data from, for example, the Mainz (Bernauer *et al.*, 2010) and Jefferson Lab (JLab) (Xiong *et al.*, 2019) electron-proton scattering measurements. For a recent review of the history and the theoretical framework of the dispersive form factor analyses, see Lin, Hammer, and Meißner (2021).

The recoil correction was considered by Karshenboim *et al.* (2015), who obtained

$$E_{\text{rec}} = 0.00003(5) \text{ meV}. \quad (91)$$

A similar result recently obtained by Tomalak (2022)

$$E_{\text{rec}} = 0.00005(1) \text{ meV} \quad (92)$$

was based on the proton form factor parametrization of Borah *et al.* (2020), who used the small proton charge radius from the μH Lamb shift as a constraint.

In total the Born contribution amounts to

$$E_{\text{Born}} = -0.0211(2) \text{ meV}. \quad (93)$$

This prediction not only is more precise but also differs from older values: $E_{\text{Born}} = -0.0186(16) \text{ meV}$ (Tomalak, 2019) and $E_{\text{Born}} = -0.0247(16) \text{ meV}$ (Birse and McGovern, 2012). To explain this, we note that Birse and McGovern (2012) and Tomalak (2019) used proton form factor parametrizations that corresponded to a large r_p . Since the value of the latter is correlated with the resulting E_{Born} , a consistent TPE evaluation should use a form factor parametrization that results in a small r_p , as argued by Karshenboim (2014). While Tomalak (2019) used a procedure suggested by Karshenboim (2014) and Karshenboim *et al.* (2015) to correct for the large radius of the A1 parametrization (Bernauer *et al.*, 2010, 2014), the comparison to Eq. (93) indicates that the suggested correction might not be sufficiently accurate.

The subtraction contribution was considered in various works (Birse and McGovern, 2012; Gorchtein, Llanes-Estrada, and Szczepaniak, 2013; Peset and Pineda, 2014; Tomalak and Vanderhaeghen, 2016; Lensky *et al.*, 2018), and we take the value

$$E_{\text{sub}} = 0.0046(24) \text{ meV} \quad (94)$$

from the most recent prediction in the framework of χPT (Lensky *et al.*, 2018). As previously mentioned, the q^2 dependence of the $T_1(0, -q^2)$ subtraction function, which is related to the magnetic dipole polarizability, has not been experimentally constrained, and its uncertainty is the largest among all contributions to the μH Lamb shift. Last, for the inelastic contribution

$$E_{\text{inel}} = -0.0127(5) \text{ meV} \quad (95)$$

we take a value of Carlson and Vanderhaeghen (2011). As a final result for the TPE with the subtracted point proton, we obtain

$$E_{\text{TPE}}(\mu\text{H}, 2S) = -0.0292(25) \text{ meV}, \quad (96)$$

with the uncertainty dominated by the one from the subtraction term. Note that, given the present uncertainties of the Friar and polarizability contributions, the recoil correction is negligible in the case of μH .

2. TPE in μD

In the case of μD , the first data-driven dispersive evaluation of the TPE correction was performed by Carlson, Gorchtein, and Vanderhaeghen (2014) with the result $E_{\text{TPE}}(\mu\text{D}, 2S) = -2.011(740) \text{ meV}$, but with an inconsistent subtraction of the point deuteron $t^{\mu\nu}$. They set $G_C = 1$ and $G_M = G_Q = 0$ for a point deuteron, whereas they should have set $G_C = G_M = 1$ and $G_Q = 0$, which would correspond to $G_1 = G_2 = 1$ and $G_3 = 0$ (in their notation) because the $(Z\alpha)^5$ recoil correction in Eq. (54) was calculated assuming these values for the elastic form factors of the point deuteron. The same formalism as was used by Carlson, Gorchtein, and Vanderhaeghen (2014) was employed in several more recent works (Acharya *et al.*, 2021; Lensky, Hagelstein, and Pascalutsa, 2022b). To make it consistent with Eq. (54), it is sufficient to modify the elastic contribution of Carlson, Gorchtein, and Vanderhaeghen (2014), as shown in Appendix A. The numerical effect of this modification turns out to be small ($\sim -0.00004 \text{ meV}$) and thus can be neglected.

A remark regarding the dispersion relation formalism is in order. The subtraction function $T_1(0, -q^2)$ is treated differently in composite nuclei than in μH . In a data-driven approach, the dominant purely nuclear response in electron-nucleus scattering can be separated from the response of the individual nucleons, leading to a finite-energy sum rule for the nuclear part of $T_1(0, -q^2)$, as shown by Gorchtein (2015). As an alternative to using data, one often utilizes the nuclear response functions calculated from a theory of nuclear interactions. In this case, there is also as a rule no need for a subtraction, at least when the theory does not yet resolve the structure of the individual nucleons. That said, the small subtraction contribution due to the individual nucleons inherits all of the difficulties of the μH case.

Most recent works use chiral effective field theories (χEFT) of nuclear interactions (Epelbaum, Hammer, and Meißner, 2009; Machleidt and Entem, 2011; Epelbaum, Krebs, and Reinert, 2020; Hammer, König, and Van Kolck, 2020) to evaluate the deuteron structure functions instead of using

experimental input, due to the lack of quality data; see the discussion given by [Acharya *et al.* \(2021\)](#). [Lensky, Hagelstein, and Pascalutsa \(2022a, 2022b\)](#) analyzed pionless effective field theory ($\not\chi$ EFT) and χ EFT predictions and pointed out that the deuteron charge form factor parametrization by the JLab t_{20} Collaboration ([Abbott *et al.*, 2000](#)) does not describe the deuteron well enough in the low q^2 region, i.e., in the region without data. The latter parametrization was employed by [Carlson, Gorchtein, and Vanderhaeghen \(2014\)](#) and [Acharya *et al.* \(2021\)](#) to evaluate the elastic TPE. Accordingly, we update the elastic part of [Acharya *et al.* \(2021\)](#) by taking the value $-0.4456(18)$ meV from Table II of [Lensky, Hagelstein, and Pascalutsa \(2022b\)](#), a result stemming from a χ EFT calculation of G_C ([Filin *et al.*, 2021](#)). For the inelastic part of [Acharya *et al.* \(2021\)](#) we take the arithmetic mean of their two results $-(1.511 + 1.519)/2$ meV and finally add their hadronic contribution -0.028 meV to obtain

$$\begin{aligned} E_{\text{TPE}}(\mu\text{D}, 2S) &= [-0.446(2) - 1.515(15) - 0.028(2)] \text{ meV} \\ &= -1.990(15) \text{ meV}. \end{aligned} \quad (97)$$

The most recent calculation by [Lensky, Hagelstein, and Pascalutsa \(2022a, 2022b\)](#) used $\not\chi$ EFT amplitudes for the forward virtual Compton scattering off the deuteron ([Lensky, Hiller Blin, and Pascalutsa, 2021](#)) to obtain a similar sum of three contributions

$$\begin{aligned} E_{\text{TPE}}(\mu\text{D}, 2S) &= [-0.446(8) - 1.509(16) - 0.032(6)] \text{ meV} \\ &= -1.987(20) \text{ meV}, \end{aligned} \quad (98)$$

which is in perfect agreement with Eq. (97). Another recent calculation ([Emmons, Ji, and Platter, 2021](#)) used $\not\chi$ EFT with pointlike nucleons to evaluate the deuteron inelastic structure functions. This calculation obtained the inelastic part of E_{TPE} [$-1.574(80)$ meV] with a larger central value (as a result of treating the nucleons as pointlike) but also a larger uncertainty, making it consistent with the other evaluations.

Regarding direct calculation of E_{TPE} from the nuclear theory, one can use an effective Hamiltonian, either phenomenological or rooted in χ EFT, and derive the TPE correction. The first such calculations were performed by [Leidemann and Rosenfelder \(1995\)](#). Later, a much improved method was introduced by [Pachucki \(2011\)](#) and expanded on by [Hernandez *et al.* \(2014\)](#), [Pachucki and Wienczek \(2015\)](#), and [Ji *et al.* \(2018\)](#), resulting in the following formula for the TPE contribution:

$$E_{\text{TPE}} = E_{\text{nuc1}} + E_{\text{nuc2}} + E_{\text{pol}} + \dots, \quad (99)$$

$$E_{\text{nuc1}} = -\frac{\pi}{3} m \alpha^2 \phi^2(0) [ZR_F^3(p) + (A - Z)R_F^3(n)], \quad (100)$$

$$E_{\text{nuc2}} = -\frac{\pi}{3} m \alpha^2 \phi^2(0) \sum_{i,j=1}^Z \langle \phi_N || \vec{r}_i - \vec{r}_j ||^3 | \phi_N \rangle, \quad (101)$$

$$E_{\text{pol}} = -\frac{4\pi\alpha^2}{3} \phi^2(0) \int_{E_T} dE \sqrt{\frac{2\mu}{E}} |\langle \phi_N || \vec{d} | E \rangle|^2, \quad (102)$$

where the Coulomb distortion correction is considered separately in Sec. V.B since it is of $(Z\alpha)^6$ order. Here E_{nuc1} is a sum of TPE contributions from each individual nucleon, E_{nuc2} is due to TPE with different nucleons, and E_{pol} is the leading nuclear polarizability correction originating from the low-energy TPE and is given by the matrix elements of the electric dipole operator $e\vec{d}$ between the nuclear ground state $|\phi_N\rangle$ and excited states $|E\rangle$, with E_T the lowest excitation energy. Note that Eq. (100) is proportional to m instead of μ , thus differing from the convention in Eq. (87). The parameters $R_F(p)$ and $R_F(n)$ are the effective proton and neutron radii, which include the complete TPE with the corresponding nucleon. The value for the proton is obtained from E_{TPE} in μH ,

$$R_F^3(p) = 2.876(246) \text{ fm}^3, \quad (103)$$

and for the neutron the value was calculated by [Tomalak \(2019\)](#),

$$R_F^3(n) = 0.712(223) \text{ fm}^3. \quad (104)$$

There are many more small corrections in the effective Hamiltonian approach for the calculation of the TPE contribution in μD ; they are denoted by dots in Eq. (99) and were separately calculated by two groups: (i) [Pachucki \(2011\)](#) and [Pachucki and Wienczek \(2015\)](#) and (ii) [Hernandez *et al.* \(2014, 2018, 2019\)](#) and [Ji *et al.* \(2018\)](#). Using the aforementioned values of $R_F(p)$ and $R_F(n)$, we update the calculation of [Pachucki and Wienczek \(2015\)](#) by changing the single-nucleon contributions [see Eqs. (45) and (46) in their paper] to $\delta_P E = -0.034(3)$ meV and $\delta_N E = -0.008(3)$ meV. Their total E_{TPE} thus becomes

$$E_{\text{TPE}}(\mu\text{D}, 2S) = -1.961(20) \text{ meV}. \quad (105)$$

Considering more elaborate calculations by the second group ([Ji *et al.*, 2018](#)), we note that the point deuteron $(Z\alpha)^5$ recoil correction was not properly subtracted but do not expect this to be significant. Therefore, we take their $\delta_{\text{TPE}}^A = [-1.675(15) - 0.262]$ meV (with the subtracted Coulomb distortion) and add the nucleon contribution $\delta_{\text{TPE}}^N = \delta_P E + \delta_N E$ to obtain

$$E_{\text{TPE}}(\mu\text{D}, 2S) = -1.979(15) \text{ meV}, \quad (106)$$

which is in agreement with the updated value in Eq. (105). As a final value we take the mean value of Eqs. (97), (98), (105), and (106) and keep the largest uncertainty

$$E_{\text{TPE}}(\mu\text{D}, 2S) = -1.979(20) \text{ meV} \quad (107)$$

to account for possible systematic uncertainties in all of these determinations; see the discussion in Sec. VI.

3. TPE in μHe^+

A calculation of E_{TPE} in $\mu^3\text{He}^+$ using the experimentally measured inelastic structure functions was performed by [Carlson, Gorchtein, and Vanderhaeghen \(2017\)](#), but with

large uncertainties. Much greater accuracy is achieved by direct nuclear structure calculations using Eqs. (99)–(102). In the case of $\mu^3\text{He}^+$ and $\mu^4\text{He}^+$, calculations of E_{TPE} were performed by Ji *et al.* (2013, 2018) and Nevo Dinur *et al.* (2016). We start with their results, which were denoted as δ_{TPE} by Ji *et al.* (2018) in their Table 7, subtract the Coulomb distortion corrections $\delta_C^{(0)}(\mu^3\text{He}^+) = 1.010$ meV and $\delta_C^{(0)}(\mu^4\text{He}^+) = 0.536$ meV, and update the single-nucleon contributions using Eqs. (103) and (104): $\delta_{\text{Zem}}^N + \delta_{\text{pol}}^N = -0.647(55)$ meV for $\mu^3\text{He}^+$ and $\delta_{\text{Zem}}^N + \delta_{\text{pol}}^N = -0.738(63)$ meV for $\mu^4\text{He}^+$. This gives

$$E_{\text{TPE}}(\mu^3\text{He}^+, 2S) = -16.38(31) \text{ meV}, \quad (108)$$

$$E_{\text{TPE}}(\mu^4\text{He}^+, 2S) = -9.76(40) \text{ meV}, \quad (109)$$

where the improvement in the accuracy with respect to the original results of Ji *et al.* (2018) is due to the updated single-nucleon contributions.

B. Coulomb distortion correction

Among corrections of higher order in α , the largest one is the Coulomb distortion correction, which comes from the expansion in the ratio of the muon binding energy to the nuclear excitation energy and is enhanced by a factor of $\ln(Z\alpha)^2$,

$$\delta_C E = \frac{Z^4 \alpha^6 \mu^4}{6} \int_{E_T} \frac{dE}{E} \left[\frac{1}{6} + \ln \left(\frac{2\mu(Z\alpha)^2}{E} \right) \right] |\langle \phi_N | \vec{d} | E \rangle|^2. \quad (110)$$

Since the first term $1/6$ in square brackets in Eq. (110) is much smaller than the logarithm, it is sometimes neglected (Ji *et al.*, 2018). This correction was calculated in a manner similar to the leading nuclear polarizability correction in Eq. (102) [see Ji *et al.* (2018) for details], with the numerical values presented in Table I.

C. Three-photon exchange

In the nonrecoil limit, the elastic three-photon exchange (3PE) contribution can be obtained by solving the Dirac equation with a finite size nucleus. The corresponding relative $O(\alpha)^2$ correction to the finite size effect can be represented as (Pachucki, Patkóš, and Yerokhin, 2018)

$$\begin{aligned} E_{\text{FNS}}^{(6)}(2S) = & -(Z\alpha)^6 m^3 r_C^2 \frac{1}{12} \left[\ln(mr_{C2} Z\alpha) + \gamma_E - \frac{31}{16} \right] \\ & + (Z\alpha)^6 m^5 r_C^4 \frac{1}{18} \left[\ln(mr_{C1} Z\alpha) + \gamma_E + \frac{5}{2} \right] \\ & + (Z\alpha)^6 m^5 r_{CC}^4 \frac{1}{480}, \end{aligned} \quad (111)$$

$$E_{\text{FNS}}^{(6)}(2P_{1/2}) = (Z\alpha)^6 m \left(\frac{m^2 r_C^2}{64} + \frac{m^4 r_{CC}^4}{480} \right), \quad (112)$$

where $r_{CC}^4 = \langle r^4 \rangle$ is the fourth moment of the charge density, the effective nuclear charge radii r_{C1} and r_{C2} encode the

high-momentum contributions, and γ_E is the Euler constant. For the exponential distribution of the nuclear charge $r_{CC}/r_C = 1.257433$, $r_{C1}/r_C = 1.090044$, and $r_{C2}/r_C = 1.068497$. The inelastic contribution is difficult to estimate. The only known result is for μD (Pachucki, Patkóš, and Yerokhin, 2018), where it was found to partially cancel the elastic part. Therefore, for other composite nuclei we assume that the total 3PE in the nonrecoil limit is half of the elastic part, with the uncertainty being the other half.

D. Electron vacuum polarization with TPE

The eVP⁽¹⁾ correction to the TPE contribution is

$$\begin{aligned} \delta E_{\text{TPE}} = & -\frac{(Ze^2)^2}{2} \phi^2(0) \int_s \frac{d^4 q}{(2\pi)^4 i q^4} [T^{\mu\nu} - \mu^\nu(I, M)] \\ & \times t_{\mu\nu}(m) \left[-2\bar{\omega}^{(1)}(q^2/m_e^2) + 2\frac{\delta\phi(0)}{\phi(0)} \right], \end{aligned} \quad (113)$$

where $\delta\phi$ is as defined in Eq. (52), $\bar{\omega}^{(1)}$ is as defined in Eq. (32), and the subscript s in the integral denotes an additional subtraction of the finite size that is the same as in Eq. (75). The eVP⁽¹⁾ correction to the elastic part in the nonrecoil limit, namely, to the Friar term, was obtained by Karshenboim *et al.* (2018). Their results were 0.0004, 0.0071, 0.212, and 0.139 meV for the Lamb shifts in μH , μD , $\mu^3\text{He}^+$, and $\mu^4\text{He}^+$, respectively. However, these results are incomplete because the eVP⁽¹⁾ correction to the inelastic part is unknown. Therefore, we do not use these results, and instead calculate the eVP⁽¹⁾ corrections to the leading contributions to E_{TPE} , namely, E_{nuc1} , E_{nuc2} , and E_{pol} in Eqs. (99)–(102). The details are presented in Appendixes B, C, and D, respectively. This largely completes the evaluation of the eVP⁽¹⁾ correction with TPE.

In particular, for μH there is only the eVP⁽¹⁾ correction with TPE on the proton, which amounts to

$$\delta E_{\text{TPE}}(\mu\text{H}) = 0.0006(1) \text{ meV} \quad (114)$$

for the Lamb shift; see Eq. (B5). For μD , the resulting correction to the Lamb shift is the sum of the single-nucleon eVP⁽¹⁾ with TPE from Eq. (B5) and the eVP⁽¹⁾ polarizability correction from Kalinowski (2019),

$$\delta E_{\text{TPE}}(\mu\text{D}) = 0.0275(4) \text{ meV}, \quad (115)$$

for the Lamb shift. This is in agreement with the calculation of the eVP⁽¹⁾ correction to TPE recently performed by Lensky, Hagelstein, and Pascalutsa (2022a, 2022b), which gave 0.0274(3) meV. Finally, for $\mu^3\text{He}^+$ and $\mu^4\text{He}^+$ we add δE_{nuc1} from Eq. (B5), δE_{nuc2} from Eq. (C11), and δE_{pol} from Eq. (D3) to obtain

$$\delta E_{\text{TPE}}(\mu^3\text{He}^+) = 0.266(24) \text{ meV}, \quad (116)$$

$$\delta E_{\text{TPE}}(\mu^4\text{He}^+) = 0.158(12) \text{ meV} \quad (117)$$

for the Lamb shift. These results are shown in Table I.

E. Muon self-energy and vacuum polarization with TPE

This correction is given by

$$\delta E_{\text{TPE}} = -\frac{(Ze^2)^2}{2} \phi^2(0) \int \frac{d^4q}{(2\pi)^4 i q^4} [T^{\mu\nu} - t^{\mu\nu}(I, M)] \times [t_{\mu\nu}^{\text{rad}}(m) - 2\bar{\omega}^{(1)}(q^2/m^2)t_{\mu\nu}(m)], \quad (118)$$

where $t_{\mu\nu}^{\text{rad}}$ is the muon self-energy correction to the pointlike $t_{\mu\nu}$ and $\bar{\omega}^{(1)}$ is the one-loop muon vacuum polarization; see Eq. (32). An analytic expression for $t_{\mu\nu}^{\text{rad}}$ is known (Pachucki, 1995), so this correction can in principle be calculated for μH and μD using the experimentally or theoretically determined nuclear amplitudes T_1 and T_2 . For μHe^+ , the most convenient approach is the direct calculation using the nuclear theory with an effective Hamiltonian; cf. Eq. (99). However, such a calculation has not yet been performed. The correction in Eq. (118) has thus far been calculated (Faustov *et al.*, 2017; Karshenboim *et al.*, 2018) in the elastic limit for an infinitely heavy nucleus with the use of different models for the charge distribution. In Appendix E, we recalculate this correction using the exponential charge distribution to obtain results in agreement with Faustov *et al.* (2017) and Karshenboim *et al.* (2018). Moreover, we note that this contribution is dominated by the mean square charge radius with the radiatively corrected muon density at the nucleus. Therefore, the inelastic contribution is not expected to be significant, and we estimate the relative uncertainties of our results in Eq. (E12) at 10%.

VI. SUMMARY

If the nuclei were pointlike particles, the $2S - 2P$ Lamb shift in light muonic atoms would be sensitive to the hVP, as the muon $g - 2$ is. A theoretical understanding of nuclear structure at the relevant level of precision remains, despite recent steady progress, a challenging matter. As a result, the theoretical predictions for the energy spectra of muonic atoms are currently a factor of 10 to ~ 100 times less accurate than what would be obtained in the pointlike limit; therefore, the sensitivity to new physics in measurements in light muonic atoms is at present limited.

The uncertainty of theoretical calculations are at present dominated by the hadronic and nuclear contributions rather than the QED terms, which can be obtained with much higher accuracy. Focusing on such dominant contributions, it is useful to distinguish between single-nucleon and few-nucleon uncertainties. The fact that the structure of the single nucleon is not well known is affecting terms such as E_{nuc1} in Eq. (99) and generates the entire uncertainty of E_{NS} in μH . Presently such theoretical uncertainty for μH is of the order of the current experimental uncertainty. Using only χPT makes it difficult to match the projected new measurements, which plan to achieve a factor of 5 improvement in the empirical uncertainty. However, there are promising developments in the data-driven approach (Tomalak and Vanderhaeghen, 2016), and lattice QCD calculations could achieve the needed precision in the future; see Fu *et al.* (2022) for the first calculation of the TPE contribution in μH . Furthermore, Hagelstein and Pascalutsa (2021) showed that the TPE

contribution can be obtained using an alternative subtraction at $T_1(iQ, Q^2)$, which holds advantages for EFT and lattice QCD calculations.

The uncertainties related to the few-nucleon dynamics start at μD and move to heavier muonic atoms. They are due to the model dependence intrinsic to the parametrization of nuclear interactions. Calculations have been performed using different nuclear potentials to allow for an estimate of the associated model dependence (Ji *et al.*, 2013, 2018; Nevo Dinur *et al.*, 2016). When the study is restricted to interactions developed within χEFT , an order-by-order analysis in the chiral expansion is necessary to estimate the uncertainty introduced in the truncation of the expansion. To date this has been achieved only for μD (Hernandez *et al.*, 2014, 2018), and work is in progress for $\mu^3\text{He}^+$ and $\mu^4\text{He}^+$ (Li Muli and Bacca, 2023). Reducing such uncertainty is difficult and can be done only either by increasing the order of the χEFT expansion or by exploring other ways of fitting the χEFT low-energy constants at the present order. Even if we were able to reduce these errors, there are other sources of uncertainty, such as corrections to Eq. (99) including higher-order polarizabilities and unknown corrections to the nuclear electric dipole operator (Wienczek, Puchalski, and Pachucki, 2014; Hernandez *et al.*, 2019; Li Muli *et al.*, 2022).

When the uncertainties stemming from single-nucleon and few-nucleon dynamics are compared for μD and μHe^+ , the two are found to be comparable in size even though the absolute contribution of terms stemming from the few-nucleon dynamics is larger; see Table 7 of Ji *et al.* (2018). Finally, another important source of uncertainty in the μHe^+ ion is the unknown inelastic part of the three-photon exchange correction; see Sec. V.C.

In view of these uncertainties, the comparison of the nuclear rms charge radii between muonic and electronic atoms would be interesting. Recent results using hydrogen spectroscopy (Beyer *et al.*, 2017; Fleurbaey *et al.*, 2018; Bezginov *et al.*, 2019; Grinin *et al.*, 2020; Brandt *et al.*, 2022), although not yet conclusive, tend to be in agreement with the μH value. The absolute determination of nuclear radii from the optical spectroscopy of normal atoms, other than hydrogen, has thus far not been successful. The only attempt from the measurement of the $2^3S - 2^3P$ transition in ^4He (Patkóš, Yerokhin, and Pachucki, 2021), although in agreement with the $\mu^4\text{He}^+$ determination, is much less accurate due to the high complexity of QED effects in systems consisting of more than one electron. On the other side, the optical spectroscopy of the one-electron He^+ ion has not yet been accomplished (Herrmann *et al.*, 2009; Krauth *et al.*, 2020).

The proton rms radius r_p extracted from the μH Lamb shift (see Table I) is by far the most accurate. Therefore, one can use this r_p for the most accurate determination of the Rydberg constant from the $1S - 2S$ hydrogen spectroscopy, for the most accurate determination of the rms deuteron charge radius r_d from the H-D isotope shift in the $1S - 2S$ transition, or recently for the most accurate determination of the electron-proton mass ratio from the precise spectroscopy of the HD^+ molecule. The Lamb shift measurements in all other muonic atoms, although they do not lead to improvements in tests of fundamental physics, can give valuable information about

electromagnetic properties of nuclei. Namely, we recall that the energy shift due to the finite nuclear size is proportional to the nuclear charge radius ($E_{\text{FNS}} = Cr_C^2$). It turns out that the weighted isotope shift in muonic atoms $E_L(\text{D})/C_{\text{D}} - E_L(\text{H})/C_{\text{H}}$, where the corresponding coefficients C are given in Table I, can be used for the determination of the difference of squared nuclear charge radii with a higher precision than the individual charge radii due to partial cancellations of uncertainties, resulting in

$$r_d^2 - r_p^2|_{\text{muonic}} = 3.8200(7)_{\text{exp}}(30)_{\text{theo}} \text{ fm}^2. \quad (119)$$

Equation (119) is in perfect agreement with the value obtained from the electronic H-D isotope shift in the $1S - 2S$ transition (Parthey *et al.*, 2010), resulting in a much more accurate determination (Pachucki, Patkóš, and Yerokhin, 2018),

$$r_d^2 - r_p^2|_{\text{electronic}} = 3.8207(3) \text{ fm}^2. \quad (120)$$

This indicates that we have a good understanding of the electromagnetic properties of the deuteron. An analogous comparison can be performed for the ^3He - ^4He isotope shift, for which we obtain

$$\frac{E_L(^4\text{He}^+)}{C_{^4\text{He}^+}} - \frac{E_L(^3\text{He}^+)}{C_{^3\text{He}^+}} = 0.2585(30) \text{ fm}^2 + r_\alpha^2 - r_h^2, \quad (121)$$

where we took advantage of the partial cancellation of uncertainties in the nuclear structure contribution E_{NS} . A recent measurement of the Lamb shift in $\mu^3\text{He}^+$ (Schuhmann *et al.*, 2023) gave

$$r_h^2 - r_\alpha^2|_{\text{muonic}} = 1.0636(6)_{\text{exp}}(30)_{\text{theo}} \text{ fm}^2. \quad (122)$$

The value (122) deviated by 3.6σ from the recent measurement of the ^3He - ^4He isotope shift in the $2^3S_1 - 2^1S_0$ transition (Van der Werf *et al.*, 2023),

$$r_h^2 - r_\alpha^2|_{\text{electronic}} = 1.0757(15) \text{ fm}^2. \quad (123)$$

We point out, however, that the other isotope shift measurements in the $2^3P_1 - 2^3S_1$ transition have thus far not been conclusive, because they are in contradiction with each other (Pachucki, Patkóš, and Yerokhin, 2017); see also Van der Werf *et al.* (2023). Therefore, we postpone drawing conclusions until measurements of the $2^3P_1 - 2^3S_1$ transition in ^3He are confirmed.

Finally, our determination of the proton, the deuteron, and the α particle charge radii differs from the original ones given by Antognini *et al.* (2013), Pohl *et al.* (2016), and Krauth *et al.* (2021) (see Table I), especially for the deuteron, while that for the helion charge radius (Schuhmann *et al.*, 2023) is based on our calculations presented here. The main reason for these differences is the neglect of the $e\text{VP}^{(1)}$ correction to the TPE and the inelastic 3PE in the original determination. Moreover, the large uncertainties in E_{NS} indicate that a more accurate calculation of the electromagnetic nuclear structure of light nuclei is necessary to explore the great potential of the precision muonic atom spectroscopy.

ACKNOWLEDGMENTS

We are grateful to S. G. Karshenboim for explanations regarding his work, and to O. Tomalak for letting us know the result of his calculation of the recoil correction in TPE with the proton. K. P. was supported by National Science Centre (Poland) Grant No. 2017/27/B/ST2/02459. F. H. and V. L. were supported by the Deutsche Forschungsgemeinschaft (DFG) through the Emmy Noether Programme under Grant No. 449369623. S. S. L. M., S. B., and R. P. were supported through the Cluster of Excellence ‘‘Precision Physics, Fundamental Interactions, and Structure of Matter’’ (PRISMA⁺ EXC 2118/1) funded by the DFG within the German Excellence Strategy (Project ID No. 390831469). R. P. acknowledges support from the European Union’s Horizon 2020 research and innovation program through the STRONG-2020 project under Grant Agreement No. 824093.

APPENDIX A: SUBTRACTION OF THE POINT DEUTERON AMPLITUDE

In this appendix we specify the changes to the covariant dispersive formalism of Carlson, Gorchtein, and Vanderhaeghen (2014) that were necessary to account for the subtraction of the point deuteron amplitude described in Sec. V.A. As explained there, Carlson, Gorchtein, and Vanderhaeghen (2014) assumed that $g = 0$ for the pointlike deuteron, whereas the definition of the latter as a Proca particle means that $g = 1$. To compensate for this difference, one needs to modify Eq. (16) of Carlson, Gorchtein, and Vanderhaeghen (2014), which describes the elastic contribution of the TPE in terms of the elastic deuteron form factors as follows:

$$\begin{aligned} E^{\text{el}} &= \frac{m \alpha^2}{M(M^2 - m^2)} \phi(0)^2 \int_0^\infty \frac{dQ^2}{Q^2} \\ &\times \left\{ \frac{2}{3} [G_M^2 - 1] (1 + \tau) \hat{\gamma}_1(\tau, \tau_l) - \frac{2}{3} (\tau - \tau_l) \frac{\gamma_1(\tau_l)}{\sqrt{\tau_l}} \right. \\ &- \left[\frac{G_C^2 - 1}{\tau} + \frac{2}{3} [G_M^2 - 1] + \frac{8}{9} \tau G_Q^2 \right] \hat{\gamma}_2(\tau, \tau_l) \\ &\left. + 16 M^2 \frac{M - m}{Q} G_C'(0) \right\}, \quad (\text{A1}) \end{aligned}$$

where $Q^2 = -q^2$, $\tau = Q^2/(4M^2)$, $\tau_l = Q^2/(4m^2)$, and the weighting functions are defined as they were by Carlson, Gorchtein, and Vanderhaeghen (2014),

$$\hat{\gamma}_{1,2}(x, y) = \frac{\gamma_{1,2}(x)}{\sqrt{x}} - \frac{\gamma_{1,2}(y)}{\sqrt{y}}, \quad (\text{A2a})$$

$$\gamma_1(x) = (1 - 2x)\sqrt{1 + x} + 2x^{3/2}, \quad (\text{A2b})$$

$$\gamma_2(x) = (1 + x)^{3/2} - x^{3/2} - \frac{3}{2}\sqrt{x}. \quad (\text{A2c})$$

Note the second term in the curly brackets in Eq. (A1) that is generated by the nonpole part of the point deuteron amplitude, and that the Thomson term still needs to be subtracted from the nonpole amplitude as it was by Carlson, Gorchtein, and Vanderhaeghen (2014). The numerical effect of the extra subtraction terms in Eq. (A1) on $E_{\text{TPE}}(\mu\text{D}, 2S)$ does not depend

on the elastic deuteron form factors and turns out to be small, namely, $-0.000\,038$ meV.

APPENDIX B: eVP⁽¹⁾ CORRECTION WITH TPE ON SINGLE NUCLEONS

In this appendix we give an improved estimate for the eVP⁽¹⁾ correction to the TPE between the muon and individual nucleons [cf. Eqs. (100) and (113)],

$$\delta E_{\text{nucl1}} = -\frac{\pi}{3} m \alpha^2 \phi^2(0) \{Z \delta[R_F^3(p)] + (A-Z) \delta[R_F^3(n)]\} + 2 \frac{\delta\phi(0)}{\phi(0)} E_{\text{nucl1}}. \quad (\text{B1})$$

For the Born TPE with an eVP⁽¹⁾ insertion, we use the nucleon form factor parametrizations from [Borah *et al.* \(2020\)](#). For the nucleon polarizability contribution with an eVP⁽¹⁾ insertion, we use the leading-order χ PT prediction plus the contribution of the $\Delta(1232)$ intermediate state (with the latter equal for p and n); see [Alarcon, Lensky, and Pascalutsa \(2014\)](#), [Lensky *et al.* \(2018\)](#), and [Lensky, Hagelstein, and Pascalutsa \(2022b\)](#). Our total results for TPE with eVP⁽¹⁾ insertion are

$$\delta[R_F^3(p)] = 0.053(10) \text{ fm}^3, \quad (\text{B2})$$

$$\delta[R_F^3(n)] = 0.017(10) \text{ fm}^3. \quad (\text{B3})$$

The wave function correction was taken from Table 13 of [Karshenboim and Shelyuto \(2021\)](#),

$$2 \frac{\delta\phi(0)}{\phi(0)} = \frac{\alpha}{\pi} \times \begin{cases} 1.4043 & \text{for } \mu\text{H}, \\ 1.4523 & \text{for } \mu\text{D}, \\ 2.1818 & \text{for } \mu^3\text{He}^+, \\ 2.1920 & \text{for } \mu^4\text{He}^+. \end{cases} \quad (\text{B4})$$

Adding it all up, we find the total eVP⁽¹⁾ correction to TPE with individual nucleons,

$$\delta E_{\text{nucl1}}(2S) = \begin{cases} -0.0006(1) & \text{meV for } \mu\text{H}, \\ -0.0010(2) & \text{meV for } \mu\text{D}, \\ -0.016(2) & \text{meV for } \mu^3\text{He}^+, \\ -0.018(3) & \text{meV for } \mu^4\text{He}^+. \end{cases} \quad (\text{B5})$$

APPENDIX C: eVP⁽¹⁾ CORRECTION WITH TPE ON DIFFERENT NUCLEONS

This derivation is based on [Pachucki and Wienczek \(2015\)](#). We now consider the muonic matrix element P for the nonrelativistic two Coulomb exchange

$$P = \langle \phi | \frac{\alpha}{|\vec{r} - \vec{r}_a|} \frac{1}{(H_0 - E_0 + E)} \frac{\alpha}{|\vec{r} - \vec{r}_b|} | \phi \rangle, \quad (\text{C1})$$

where E is the nuclear excitation energy. Using the on-mass-shell approximation and subtracting the point Coulomb exchange, Eq. (C1) becomes

$$P = \alpha^2 \phi^2(0) \int \frac{d^3k}{(2\pi)^3} \left(\frac{4\pi}{k^2} \right)^2 \left(E + \frac{k^2}{2\mu} \right)^{-1} \times (e^{i\vec{k} \cdot (\vec{r}_a - \vec{r}_b)} - 1). \quad (\text{C2})$$

We now calculate the expansion coefficients in powers of E . There are two characteristic integration regions: $|\vec{k}| \sim \sqrt{Em}$ and $|\vec{k}| \sim m$. In the first integration region, where $|\vec{k}|$ is small, one performs an expansion of the exponent in powers of $\vec{k} \cdot (\vec{r}_a - \vec{r}_b)$. The leading quadratic term is the electric dipole contribution

$$P_{\text{low}} = \frac{4\pi}{3} \alpha^2 \phi^2(0) \sqrt{\frac{2\mu}{E}} \vec{r}_a \cdot \vec{r}_b, \quad (\text{C3})$$

which gives E_{pol} in Eq. (102). In the second integration region, where $|\vec{k}| \sim m$ is large, one performs an expansion in powers not exactly of E but of the total nuclear energy \tilde{E} ,

$$\tilde{E} = E + \frac{k^2}{2M}. \quad (\text{C4})$$

The first expansion term after integration over \vec{k} is

$$P_{\text{high}} = \frac{\pi}{3} m \alpha^2 \phi^2(0) |\vec{r}_a - \vec{r}_b|^3, \quad (\text{C5})$$

and the corresponding correction to the energy is E_{nucl2} in Eq. (101).

To obtain the eVP⁽¹⁾ correction to E_{nucl2} , we modify one of the Coulomb propagators in Eq. (C2), subtract the finite size with the leading polarizability

$$\delta P = \alpha^2 \phi^2(0) \int \frac{d^3k}{(2\pi)^3} \left(\frac{4\pi}{k^2} \right)^2 \frac{2m}{k^2} [-2\bar{\omega}^{(1)}(-k^2/m_e^2)] \times \{e^{i\vec{k} \cdot (\vec{r}_a - \vec{r}_b)} - 1 + [\vec{k} \cdot (\vec{r}_a - \vec{r}_b)]^2/2\}, \quad (\text{C6})$$

and use the large- $|\vec{k}|$ behavior of $\bar{\omega}^{(1)}$,

$$\bar{\omega}^{(1)}(-k^2/m_e^2) \approx \frac{\alpha}{3\pi} \left(5 - \ln \frac{k^2}{m_e^2} \right), \quad (\text{C7})$$

to obtain

$$\delta P = -\frac{4}{9} m \alpha^3 \phi^2(0) |\vec{r}_a - \vec{r}_b|^3 \left[\frac{5}{12} + \ln(m_e |\vec{r}_a - \vec{r}_b|) + \gamma_E \right]. \quad (\text{C8})$$

The corresponding correction to the energy is

$$\delta E_{\text{nucl2}} = 2 \frac{\delta\phi(0)}{\phi(0)} E_{\text{nucl2}} - \sum_{a,b} \langle \delta P \rangle = E_{\text{nucl2}} \left[2 \frac{\delta\phi(0)}{\phi(0)} - \frac{\alpha}{\pi} \frac{4}{3} \left(\frac{5}{12} + \ln(m_e r_L) + \gamma_E \right) \right], \quad (\text{C9})$$

where r_L is defined by

$$\sum_{a,b} \langle |\vec{r}_a - \vec{r}_b|^3 \ln |\vec{r}_a - \vec{r}_b| \rangle = \sum_{a,b} \langle |\vec{r}_a - \vec{r}_b|^3 \rangle \ln r_L. \quad (\text{C10})$$

To estimate $\delta E_{\text{nucl}2}$, we assume that $r_L \approx 2r_C$, use the result of [Ji *et al.* \(2018\)](#) for $\delta_{R3}^{(1)} = E_{\text{nucl}2}(2S) = -8.625$ and -3.580 meV for $\mu^3\text{He}^+$ and $\mu^4\text{He}^+$, respectively, and obtain

$$\delta E_{\text{nucl}2}(2S) = \begin{cases} -0.140 \text{ (21) meV} & \text{for } \mu^3\text{He}^+, \\ -0.060 \text{ (10) meV} & \text{for } \mu^4\text{He}^+, \end{cases} \quad (\text{C11})$$

where the relative uncertainties of 15% and 16% for $\mu^3\text{He}^+$ and $\mu^4\text{He}^+$ result from the uncertainties of the adopted values of $E_{\text{nucl}2}$ and r_L (2% and 15% for $\mu^3\text{He}^+$; 5% and 15% for $\mu^4\text{He}^+$) summed in quadrature.

APPENDIX D: eVP⁽¹⁾ CORRECTION WITH THE LEADING POLARIZABILITY

The derivation is based on the work of [Kalinowski \(2019\)](#). We now consider the leading polarizability in Eq. (102) that comes from the TPE

$$E_{\text{pol}} = -\frac{4\pi\alpha^2}{3}\phi^2(0) \int_{E_T} dE |\langle \phi_N | \vec{d} | E \rangle|^2 \sqrt{\frac{2\mu}{E}}. \quad (\text{D1})$$

The eVP⁽¹⁾ correction modifies one of the photon propagators, which leads to a complicated expression. When the smallness of the parameter $m_e/\sqrt{E\mu}$ is taken into account, the first two terms in its expansion are

$$\begin{aligned} \delta E_{\text{pol}} = & -\frac{8\alpha^3}{9}\phi^2(0) \int_{E_T} dE |\langle \phi_N | \vec{d} | E \rangle|^2 \sqrt{\frac{2\mu}{E}} \\ & \times \left[\ln\left(\frac{2\mu E}{m_e^2}\right) - \frac{5}{3} + \frac{3\pi}{2} \sqrt{\frac{m_e^2}{2\mu E}} \right] + 2\frac{\delta\phi(0)}{\phi(0)} E_{\text{pol}}, \end{aligned} \quad (\text{D2})$$

where the last term comes from the eVP⁽¹⁾ correction to the wave function. [Kalinowski \(2019\)](#) obtained for μD the value $\delta E_{\text{pol}}(2S) = -0.0265(3)$ meV. Using the wave function correction from Eq. (B5) and performing calculations with the Argonne *v18* potential ([Wiringa, Stoks, and Schiavilla, 1995](#)), we obtain $\delta E_{\text{pol}}(2S) = -0.0263$ meV, which is in agreement with the aforementioned result. Following the calculation by [Ji *et al.* \(2018\)](#) of the leading polarizability with including the Urbana IX three-body force, we obtain ([Li Muli and Bacca, 2023](#))

$$\delta E_{\text{pol}}(2S) = \begin{cases} -0.110 \text{ (11) meV} & \text{for } \mu^3\text{He}^+, \\ -0.080 \text{ (6) meV} & \text{for } \mu^4\text{He}^+, \end{cases} \quad (\text{D3})$$

where the relative uncertainty for $\mu^4\text{He}^+$ is 7%, distributed as follows: 3% from the missing multipoles, 5% from the nuclear model, and 4% from the numerical evaluation. For $\mu^3\text{He}^+$, the relative uncertainty is 10%, which comes mostly from the missing multipoles (9%), with smaller additional uncertainties of 2% from the nuclear model and 4% from the numerical evaluation.

APPENDIX E: $\mu\text{SE}^{(1)} + \mu\text{VP}^{(1)}$ CORRECTION WITH THE ELASTIC TPE

This derivation is based on the work of [Pachucki \(1993\)](#). In the limit of an infinite mass nucleus, the elastic TPE with $\mu\text{SE}^{(1)} + \mu\text{VP}^{(1)}$ corrections and point-nucleus subtraction reads

$$\delta E_{\text{TPE}} = \frac{\alpha\phi^2(0)}{\pi m^2} \int \frac{d^3p}{(2\pi)^3} \frac{(4\pi\alpha)^2}{p^4} f(p^2) [\rho(p^2)^2 - 1], \quad (\text{E1})$$

where ρ is the nuclear charge form factor, $f(p^2)$ is the radiatively corrected muon line at the momentum exchange $p^0 = 0$ [see Eq. (118)],

$$\frac{\alpha}{\pi} f(p^2) = \frac{1}{2} t_{00}^{\text{rad}} + \frac{4}{p^2} \bar{\omega}^{(1)}(p^2), \quad (\text{E2})$$

and all momenta are in the muon mass units. $f(p^2)$ was calculated by [Pachucki \(1993\)](#) using dispersion relations,

$$f(p^2) = -\int_0^\infty d(q^2) \frac{f^A(q^2)}{q^2 + p^2}, \quad (\text{E3})$$

with

$$\begin{aligned} f^A(q^2) = & \frac{q^2}{4} \left(\frac{1}{1+q^2} - J^A \right) + \left(\frac{4}{q^2} + 1 \right) (J^A - 1) \\ & + \Theta(q-2) \left(\frac{4}{q^2} + 1 \right) \left(\frac{1}{q^2 \sqrt{1-4/q^2}} + \sqrt{1-\frac{4}{q^2}} \right) \\ & + \frac{4}{3} \Theta(q-2) \sqrt{1-\frac{4}{q^2}} \frac{1}{q^2} \left(1 + \frac{2}{q^2} \right), \end{aligned} \quad (\text{E4})$$

where the last term comes from μVP and

$$J^A = \frac{1}{q} \left[\arctan(q) - \Theta(q-2) \arccos\left(\frac{2}{q}\right) \right]. \quad (\text{E5})$$

Using Eq. (E3), one can transform δE_{TPE} into

$$\delta E_{\text{TPE}} = \frac{\alpha\phi^2(0)}{\pi m^2} \frac{(4\pi\alpha)^2}{2\pi^2} \int_0^\infty d(q^2) f^A(q^2) g(q), \quad (\text{E6})$$

where

$$g(q) = \int_0^\infty dp \frac{1}{p^2(q^2 + p^2)} [1 - \rho(p^2)]. \quad (\text{E7})$$

When one assumes a dipole parametrization of the electric form factor

$$\rho(p^2) = \frac{\Lambda^4}{(\Lambda^2 + p^2)^2}, \quad (\text{E8})$$

$g(q)$ becomes

$$g(q) = \frac{\pi}{16q} h(q), \quad (\text{E9})$$

where

$$h(q) = \frac{\Lambda^2}{(\Lambda + q)^4} + \frac{4\Lambda}{(\Lambda + q)^3} + \frac{19}{2(\Lambda + q)^2} + \frac{35}{2\Lambda(\Lambda + q)}. \quad (\text{E10})$$

Finally, the correction to the energy

$$\delta E_{\text{TPE}} = \alpha(Z\alpha)^2 \frac{\phi^2(0)}{m^2} \int_0^\infty dq h(q) f^A(q^2) \quad (\text{E11})$$

is integrated numerically with $\Lambda = 2\sqrt{3}\lambda_\mu/r_C$, $r_p = 0.841$ fm, $r_d = 2.127$ fm, $r_h = 1.969$ fm, and $r_\alpha = 1.678$ fm to obtain

$$\delta E_{\text{TPE}}(2S) = \begin{cases} -0.0004 & \text{meV for } \mu\text{H,} \\ -0.0026(3) & \text{meV for } \mu\text{D,} \\ -0.077(8) & \text{meV for } \mu^3\text{He,} \\ -0.059(6) & \text{meV for } \mu^3\text{He,} \end{cases} \quad (\text{E12})$$

where we have assumed a 10% uncertainty due to the elastic approximation. These results are presented in Table I.

REFERENCES

- Abbott, D., *et al.* (JLAB t20 Collaboration), 2000, *Eur. Phys. J. A* **7**, 421.
- Acharya, B., V. Lensky, S. Bacca, M. Gorchtein, and M. Vanderhaeghen, 2021, *Phys. Rev. C* **103**, 024001.
- Alarcon, J. M., V. Lensky, and V. Pascalutsa, 2014, *Eur. Phys. J. C* **74**, 2852.
- Alighanbari, S., G. S. Giri, F. L. Constantin, V. I. Korobov, and S. Schiller, 2020, *Nature (London)* **581**, 152.
- Antognini, A., F. Kottmann, F. Biraben, P. Indelicato, F. Nez, and R. Pohl, 2013, *Ann. Phys. (N.Y.)* **331**, 127.
- Antognini, A., *et al.*, 2013, *Science* **339**, 417.
- Barbieri, R., M. Caffo, and E. Remiddi, 1973, *Lett. Nuovo Cimento* **7**, 60.
- Belushkin, M. A., H. W. Hammer, and U. G. Meißner, 2007, *Phys. Rev. C* **75**, 035202.
- Berestetskii, V. B., E. M. Lifshitz, and L. P. Pitaevskii, 1982, *Quantum Electrodynamics*, 2nd ed. (Butterworth-Heinemann, Oxford).
- Bernauer, J. C., *et al.* (A1 Collaboration), 2010, *Phys. Rev. Lett.* **105**, 242001.
- Bernauer, J. C., *et al.* (A1 Collaboration), 2014, *Phys. Rev. C* **90**, 015206.
- Bethe, H. A., and E. E. Salpeter, 1977, *Quantum Mechanics of One- and Two-Electron Atoms* (Plenum, New York).
- Beyer, A., *et al.*, 2017, *Science* **358**, 79.
- Bezginov, N., T. Valdez, M. Horbatsch, A. Marsman, A. C. Vutha, and E. A. Hessels, 2019, *Science* **365**, 1007.
- Birse, M. C., and J. A. McGovern, 2012, *Eur. Phys. J. A* **48**, 120.
- Borah, K., R. J. Hill, G. Lee, and O. Tomalak, 2020, *Phys. Rev. D* **102**, 074012.
- Borie, E., and G. A. Rinker, 1978, *Phys. Rev. A* **18**, 324.
- Borie, E., and G. A. Rinker, 1982, *Rev. Mod. Phys.* **54**, 67.
- Brandt, A. D., S. F. Cooper, C. Raso, Z. Burkley, D. C. Yost, and A. Matveev, 2022, *Phys. Rev. Lett.* **128**, 023001.
- Carlson, C. E., 2015, *Prog. Part. Nucl. Phys.* **82**, 59.
- Carlson, C. E., M. Gorchtein, and M. Vanderhaeghen, 2014, *Phys. Rev. A* **89**, 022504.
- Carlson, C. E., M. Gorchtein, and M. Vanderhaeghen, 2017, *Phys. Rev. A* **95**, 012506.
- Carlson, C. E., and M. Vanderhaeghen, 2011, *Phys. Rev. A* **84**, 020102.
- Chambers, E. E., and R. Hofstadter, 1956, *Phys. Rev.* **103**, 1454.
- Diepold, M., B. Franke, J. J. Krauth, A. Antognini, F. Kottmann, and R. Pohl, 2018, *Ann. Phys. (N.Y.)* **396**, 220.
- Drake, G. W., 2023, *Springer Handbook of Atomic, Molecular, and Optical Physics*, Springer Handbooks (Springer, Cham, Switzerland).
- Dyson, F. J., 1965, *Science* **150**, 588.
- Eides, M. I., H. Grotch, and V. A. Shelyuto, 2001, *Phys. Rep.* **342**, 63.
- Emmons, S. B., C. Ji, and L. Platter, 2021, *J. Phys. G* **48**, 035101.
- Epelbaum, E., H.-W. Hammer, and U.-G. Meißner, 2009, *Rev. Mod. Phys.* **81**, 1773.
- Epelbaum, E., H. Krebs, and P. Reinert, 2020, *Front. Phys.* **8**, 98.
- Erickson, G. W., 1977, *J. Phys. Chem. Ref. Data* **6**, 831.
- Faustov, R. N., A. P. Martynenko, F. A. Martynenko, and V. V. Sorokin, 2017, *Phys. Lett. B* **775**, 79.
- Filin, A. A., D. Möller, V. Baru, E. Epelbaum, H. Krebs, and P. Reinert, 2021, *Phys. Rev. C* **103**, 024313.
- Fleurbaey, H., S. Galtier, S. Thomas, M. Bonnaud, L. Julien, F. Biraben, F. Nez, M. Abgrall, and J. Guéna, 2018, *Phys. Rev. Lett.* **120**, 183001.
- Franke, B., J. J. Krauth, A. Antognini, M. Diepold, F. Kottmann, and R. Pohl, 2017, *Eur. Phys. J. D* **71**, 341.
- Fu, Y., X. Feng, L.-C. Jin, and C.-F. Lu, 2022, *Phys. Rev. Lett.* **128**, 172002.
- Gorchtein, M., 2015, *Phys. Rev. Lett.* **115**, 222503.
- Gorchtein, M., F. J. Llanes-Estrada, and A. P. Szczepaniak, 2013, *Phys. Rev. A* **87**, 052501.
- Grinin, A., A. Matveev, D. C. Yost, L. Maisenbacher, V. Wirthl, R. Pohl, T. W. Hänsch, and T. Udem, 2020, *Science* **370**, 1061.
- Hagelstein, F., and V. Pascalutsa, 2021, *Nucl. Phys. A* **1016**, 122323.
- Hammer, H.-W., S. König, and U. van Kolck, 2020, *Rev. Mod. Phys.* **92**, 025004.
- Hernandez, O. J., A. Ekström, N. Nevo Dinur, C. Ji, S. Bacca, and N. Barnea, 2018, *Phys. Lett. B* **778**, 377.
- Hernandez, O. J., C. Ji, S. Bacca, and N. Barnea, 2019, *Phys. Rev. C* **100**, 064315.
- Hernandez, O. J., C. Ji, S. Bacca, N. Nevo Dinur, and N. Barnea, 2014, *Phys. Lett. B* **736**, 344.
- Herrmann, M., *et al.*, 2009, *Phys. Rev. A* **79**, 052505.
- Itzykson, C., and J. B. Zuber, 1980, *Quantum Field Theory*, International Series in Pure and Applied Physics (McGraw-Hill, New York).
- Ivanov, V. G., E. Y. Korzinin, and S. G. Karshenboim, 2009, *Phys. Rev. D* **80**, 027702.
- Jentschura, U., and K. Pachucki, 1996, *Phys. Rev. A* **54**, 1853.
- Jentschura, U. D., 2011a, *Eur. Phys. J. D* **61**, 7.
- Jentschura, U. D., 2011b, *Phys. Rev. A* **84**, 012505.
- Jentschura, U. D., and B. J. Wundt, 2011, *Eur. Phys. J. D* **65**, 357.
- Ji, C., S. Bacca, N. Barnea, O. J. Hernandez, and N. Nevo-Dinur, 2018, *J. Phys. G* **45**, 093002.
- Ji, C., N. Nevo Dinur, S. Bacca, and N. Barnea, 2013, *Phys. Rev. Lett.* **111**, 143402.
- Kalinowski, M., 2019, *Phys. Rev. A* **99**, 030501.
- Källén, A. O. G., and A. Sabry, 1955, *K. Dan. Vidensk. Selsk., Mat.-Fys. Medd.* **29**, 1.
- Karshenboim, S. G., 2014, *Phys. Rev. D* **90**, 053012.
- Karshenboim, S. G., V. G. Ivanov, E. Y. Korzinin, and V. A. Shelyuto, 2010, *Phys. Rev. A* **81**, 060501.

- Karshenboim, S. G., E. Y. Korzinin, V. A. Shelyuto, and V. G. Ivanov, 2015, *Phys. Rev. D* **91**, 073003.
- Karshenboim, S. G., E. Y. Korzinin, V. A. Shelyuto, and V. G. Ivanov, 2018, *Phys. Rev. A* **98**, 062512.
- Karshenboim, S. G., and V. A. Shelyuto, 2021, *Eur. Phys. J. D* **75**, 49.
- Kinoshita, T., 1990, *Quantum Electrodynamics* (World Scientific, Singapore).
- Kinoshita, T., and M. Nio, 1999, *Phys. Rev. Lett.* **82**, 3240.
- Kinoshita, T., and M. Nio, 2009, *Phys. Rev. Lett.* **103**, 079901.
- Kortunov, I. V., S. Alighanbari, M. G. Hansen, G. S. Giri, V. I. Korobov, and S. Schiller, 2021, *Nat. Phys.* **17**, 569.
- Korzinin, E. Y., V. G. Ivanov, and S. G. Karshenboim, 2013, *Phys. Rev. D* **88**, 125019.
- Krauth, J. J., M. Diepold, B. Franke, A. Antognini, F. Kottmann, and R. Pohl, 2016, *Ann. Phys. (N.Y.)* **366**, 168.
- Krauth, J. J., L. S. Dreissen, C. Roth, E. L. Gründeman, M. Collombon, M. Favier, and K. S. E. Eikema, 2020, *Proc. Sci. FFK2019*, 049 [arXiv:1910.13192].
- Krauth, J. J., *et al.*, 2021, *Nature (London)* **589**, 527.
- Krutov, A. A., A. P. Martynenko, G. A. Martynenko, and R. N. Faustov, 2015, *J. Exp. Theor. Phys.* **120**, 73.
- Lamb, W. E., and R. C. Retherford, 1947, *Phys. Rev.* **72**, 241.
- Lee, T. D., and C.-N. Yang, 1962, *Phys. Rev.* **128**, 885.
- Leidemann, W., and R. Rosenfelder, 1995, *Phys. Rev. C* **51**, 427.
- Lensky, V., F. Hagelstein, and V. Pascalutsa, 2022a, *Phys. Lett. B* **835**, 137500.
- Lensky, V., F. Hagelstein, and V. Pascalutsa, 2022b, *Eur. Phys. J. A* **58**, 224.
- Lensky, V., F. Hagelstein, V. Pascalutsa, and M. Vanderhaeghen, 2018, *Phys. Rev. D* **97**, 074012.
- Lensky, V., A. Hiller Blin, and V. Pascalutsa, 2021, *Phys. Rev. C* **104**, 054003.
- Li Muli, S. S., B. Acharya, O. J. Hernandez, and S. Bacca, 2022, *J. Phys. G* **49**, 105101.
- Li Muli, S. S., and S. Bacca, 2023 (unpublished).
- Lin, Y.-H., H.-W. Hammer, and U.-G. Meißner, 2021, *Eur. Phys. J. A* **57**, 255.
- Lin, Y.-H., H.-W. Hammer, and U.-G. Meißner, 2022, *Phys. Rev. Lett.* **128**, 052002.
- Lorenz, I. T., U.-G. Meißner, H. W. Hammer, and Y. B. Dong, 2015, *Phys. Rev. D* **91**, 014023.
- Lorenzon, W., 2020, *Proc. Sci. NuFact2019*, 076.
- Machleidt, R., and D. R. Entem, 2011, *Phys. Rep.* **503**, 1.
- Martynenko, A. P., A. A. Krutov, and R. N. Shamsutdinov, 2014, *Phys. At. Nucl.* **77**, 786.
- Mergell, P., U.-G. Meißner, and D. Drechsel, 1996, *Nucl. Phys.* **A596**, 367.
- Mohr, P. J., B. N. Taylor, and D. B. Newell, 2008, *Rev. Mod. Phys.* **80**, 633.
- Nevo Dinur, N., C. Ji, S. Bacca, and N. Barnea, 2016, *Phys. Lett. B* **755**, 380.
- Pachucki, K., 1993, *Phys. Rev. A* **48**, 120.
- Pachucki, K., 1995, *Phys. Rev. A* **52**, 1079.
- Pachucki, K., 1996, *Phys. Rev. A* **53**, 2092.
- Pachucki, K., 1999, *Phys. Rev. A* **60**, 3593.
- Pachucki, K., 2011, *Phys. Rev. Lett.* **106**, 193007.
- Pachucki, K., and H. Grotch, 1995, *Phys. Rev. A* **51**, 1854.
- Pachucki, K., and S. G. Karshenboim, 1995, *J. Phys. B* **28**, L221.
- Pachucki, K., V. Patkóš, and V. Yerokhin, 2017, *Phys. Rev. A* **95**, 062510.
- Pachucki, K., V. Patkóš, and V. A. Yerokhin, 2018, *Phys. Rev. A* **97**, 062511.
- Pachucki, K., and A. Wienczek, 2015, *Phys. Rev. A* **91**, 040503.
- Pachucki, K., and V. A. Yerokhin, 2023, *Phys. Rev. Lett.* **130**, 053002.
- Parthey, C. G., A. Matveev, J. Alnis, R. Pohl, T. Udem, U. D. Jentschura, N. Kolachevsky, and T. W. Hänsch, 2010, *Phys. Rev. Lett.* **104**, 233001.
- Parthey, C. G., *et al.*, 2011, *Phys. Rev. Lett.* **107**, 203001.
- Patkóš, V., V. A. Yerokhin, and K. Pachucki, 2021, *Phys. Rev. A* **103**, 042809.
- Patra, S., M. Germann, J. P. Karr, M. Haidar, L. Hilico, V. I. Korobov, F. M. J. Cozijn, K. S. E. Eikema, W. Ubachs, and J. C. J. Koelemeij, 2020, *Science* **369**, 1238.
- Peset, C., and A. Pineda, 2014, *Nucl. Phys.* **B887**, 69.
- Peset, C., and A. Pineda, 2015a, *Eur. Phys. J. A* **51**, 32.
- Peset, C., and A. Pineda, 2015b, *Eur. Phys. J. A* **51**, 156.
- Pohl, R., R. Gilman, G. A. Miller, and K. Pachucki, 2013, *Annu. Rev. Nucl. Part. Sci.* **63**, 175.
- Pohl, R., *et al.*, 2010, *Nature (London)* **466**, 213.
- Pohl, R., *et al.*, 2017, *Metrologia* **54**, L1.
- Pohl, R., *et al.* (CREMA Collaboration), 2016, *Science* **353**, 669.
- Salpeter, E. E., 1952, *Phys. Rev.* **87**, 328.
- Schuhmann, K., *et al.* (CREMA Collaboration), 2023, arXiv:2305.11679.
- Shabaev, V. M., 1998, *Phys. Rev. A* **57**, 59.
- Shelyuto, V. A., E. Y. Korzinin, and S. G. Karshenboim, 2018, *Phys. Rev. D* **97**, 096016.
- Shelyuto, V. A., E. Y. Korzinin, and S. G. Karshenboim, 2019, *Eur. Phys. J. D* **73**, 23.
- Tiesinga, E., P. J. Mohr, D. B. Newell, and B. N. Taylor, 2021, *Rev. Mod. Phys.* **93**, 025010.
- Tomalak, O., 2019, *Eur. Phys. J. A* **55**, 64.
- Tomalak, O., 2022 (private communication).
- Tomalak, O., and M. Vanderhaeghen, 2016, *Eur. Phys. J. C* **76**, 125.
- van der Werf, Y., K. Steinebach, R. Jannin, H. L. Bethlem, and K. S. E. Eikema, 2023, arXiv:2306.02333.
- Veitia, A., and K. Pachucki, 2004, *Phys. Rev. A* **69**, 042501.
- Wienczek, A., M. Puchalski, and K. Pachucki, 2014, *Phys. Rev. A* **90**, 022508.
- Wiringa, R. B., V. G. J. Stoks, and R. Schiavilla, 1995, *Phys. Rev. C* **51**, 38.
- Xiong, W., *et al.*, 2019, *Nature (London)* **575**, 147.